January 2018

# A Study Of Two-Phase Flow Regime And Pressure Drop In Vertical Pipe

Yanbo Wang

# A STUDY OF TWO-PHASE FLOW REGIME AND PRESSURE DROP IN VERTICAL PIPE

By

Yanbo Wang

Bachelor of Science, Liaoning Shihua University, 2015

A Thesis

Submitted to Graduate Faculty

Of the

University of North Dakota

In partial fulfillment of the requirements

For the degree of

Master of Science

Grand Forks, North Dakota

December

2018

This thesis, submitted by Yanbo Wang in partial fulfillment of the requirements for the Degree of Master of Science from the University of North Dakota, has been read by the Faculty Advisory Committee under whom the work has been done and is hereby approved.

Kegang Ling
Chairperson (Kegang Ling)

Committee Member (Hui Pu)

Committee Member (Caixia Yang)

This thesis is being submitted by the appointed advisory committee as having met all of the requirements of the School of Graduate Studies at the University of North Dakota and is hereby approved.

Wayne Swisher
Dean of the School of Graduate Studies

12/5/18
Date

PERMISSION

Title: A Study of Two-Phase Flow Regime and Pressure Drop in Vertical Pipe

Department Petroleum Engineering

Degree Master of Science

In presenting this thesis in partial fulfillment of the requirements for a graduate degree from the University of North Dakota, I agree that the library of this University shall make it freely available for inspection. I further agree that permission for extensive copying for scholarly purposes may be granted by the professor who supervised my work or, in his absence, by the Chairperson of the department or the dean of the School of Graduate Studies. It is understood that any copying or publication or other use of this thesis or part thereof for financial gain shall not be allowed without my written permission. It is also understood that due recognition shall be given to me and to the University of North Dakota in any scholarly use which may be made of any material in my thesis

Yanbo Wang

December 2, 2018

## TABLE OF CONTENTS

## LIST OF FIGURES

Figure page

## LIST OF TABLES

Table page

## ACKNOWLEDGMENTS

I wish to express my sincere appreciation to the members of my advisory Committee members, Dr. Kegang Ling, Dr. Hui Pu, and Dr. Caixia Yang for their guidance and encouragement during my time in the master's program at the University of North Dakota. I would especially like to thank my advisor Dr. Kegang Ling for invaluable advice throughout the design of experiment. A special thank you to Dr. Vamegh. Rasouli for his help to give me this opportunity to study here and financial support to design this experiment.

Finally, I would like to thank my Mom and Dad for unfailing support and encouragement throughout this challenging process.

To my mom Yu Jin and my dad Rongming Wang,
The world's best parents!

## ABSTRACT

In the oil industry, after the wellbore is drilled into a reservoir, oil and gas will flow into the bore hole and can be transported to the earth's surface through tubing. Multiphase flow will take place in the pipe. Flow regime has a significant influence on production. For example, the slug flow will cause a huge pressure-drop in the surface system and can even cause a shut-down of the well. Therefore, it is important to test two-phase upwards flow in the pipe.

Different kinds of characteristics are used to distinguish between different kinds of flow patterns. I introduce the development of flow pattern and some methods which were applied to select and determine essential parameters, such as volume fluxes rate, fluid density, viscosity, and surface tension to classify flow regime. The pressure change in the vertical tube is a summation of three factors: friction and liquid-gas interface, gravity, acceleration changing. And making an explain of the pressure drop in sucker rod pumping systems, friction force due to the movement of the plunger and the rod, buoyant force, and gravity force are including in the model.

In order to test flow regime changing and pressure-drop in two-phase upwards flow. I created a two-phase flow loop experiment, and choose to use different diameter tubes to have a comparison. The water and air flow velocities range from 0.01 to 20 m/s and 0.05 to 10 m/s, separately. I also set up a model in Ansys-Fluent to simulate the pressure drop and flow regime change in the test tube. With the comparison of the simulation result and the real experiment. The pressure-drop depends on both the diameter changing and water/air inlet superficial velocities, both of the results are coincide.

CHAPTER

# I. INTRODUCTION

## Two-phase flow in wellbore

Flow pattern has a significant influence in petroleum industry. Most of the wells were thousands of feet away from the surface. Before the oil arrives at the surface, it will go through different kinds of pattern which could result in different pressure drops.

With a large number of experiments, scholars have already concluded four kinds of flow regimes which are widely acknowledged: bubble flow, slug flow, churn flow, and annular flow. The flow patterns are easily recognized by visual inspection. As the technology is developed, many people began to use different parameters to get their own flow maps, like volume fluxes rate, fluid density, viscosity, and surface tension. There are many kinds of methods to distinguish flow patterns. However, from bubble flow to slug flow we still do not know the exact boundary. I introduce the development of flow pattern and some methods which were applied to select and determine essential parameters to classify flow regime. Some scholars have found when the void fraction between 0.25-0.3, bubbles begin to coalesce with each other and Taylor bubble emerges which is the prerequisite for the transition from bubble flow to slug flow. In testing the boundary of the pattern system from bubble flow to slug flow, the transition from bubble flow to slug flow was determined by the progress of bubble agglomeration and coalescence or break up. I follow other experiments in using multiple diameter tubes with air-water system to test the

boundary of the pattern system from bubble flow to slug flow. The regime become unstable when approaching the boundary and this instability finally causes a transition to another flow pattern.

**The Development of Flow pattern map**

The Baker's map (Baker, 1954) [1] is one of the most widely used maps. In Baker map, they used the λ and ψ parameters to take into account the properties of different gases and liquids.

$$\text{X-axes: } \frac{L*\lambda*\psi}{G} \tag{1.1}$$

$$\text{Y-axes: } \frac{G}{\lambda} \tag{1.2}$$

$$L = \frac{m_L}{S} \tag{1.3}$$

$$G = \frac{m_G}{S} \tag{1.4}$$

$$\lambda = \left[\frac{\rho_G}{\rho_{air}} * \frac{\rho_L}{\rho_W}\right]^{1/2} \tag{1.5}$$

$$\varphi = \frac{\sigma_w}{\sigma_L}\left[\frac{\mu_L}{\mu_W}\left(\frac{\rho_w}{\rho_L}\right)^2\right]^{1/3} \tag{1.6}$$

where:

$\sigma_w = 73\ dyn/cm$ : Superficial tension of the water

$\mu_W = 1\ cp$: The dynamic viscosity of water

$\rho_G$, $\rho_L$: Density of gas and liquid respectively

Golan and Stenning (Golan and Stenning, 1969) [2] presented their vertical downward flow map and upward flow map based on an air-water system test tube with the length of 3 m and 3.81 cm in diameter. They simply used the superficial velocities as coordinates.

Shell (Shell Company, 2007) [3] has created a map for transportation of combustibles. This map based on the data of gas and liquid Froude number also is determine by diameter of the pipe and the fluid velocity. The pipe diameter is 500 mm.

Gas Froude number: $F_{rG} = u_G \sqrt{\frac{\rho_g}{(\rho_l - \rho_g) g D}}$ (1.7)

Liquid Froude number: $F_{rL} = u_L \sqrt{\frac{\rho_l}{(\rho_l - \rho_g) g D}}$ (1.8)

Superficial velocity of gas: $u_g = \frac{Q_g}{(\pi D^2 / 4)} \ m/s$ (1.9)

Superficial velocity of liquid: $u_l = \frac{Q_l}{(\pi D^2 / 4)} \ m/s$ (1.10)

where:

D: The inner diameter of the pipeline

Oshinowo-Charles (Oshinowo and Charles, 1974) [4] describe the flow patterns depend on the volumetric flow rate. The length of test tube they used is 5.273m and the diameter is 2.54cm.

Properties used in the experiment:

$R_v = \frac{Q_G}{Q_L} = \frac{u_G}{u_L}$ (1.11)

$F_{rTP} = \frac{(u_G + u_L)^2}{g * D}$ (1.12)

where:

$Q_G$: The volumetric flow rate of the gas

$Q_L$: The volumetric flow rate of the liquid

$F_{rTP}$: The Froude number of the two phases

$u_G, u_L$: The gas and liquid superficial velocities respectively

**Flow pattern definition for vertical flow**

For vertical flow, Hewitt and Robert's (1969) [5] flow regime map is widely used. It bases on momentum flux to classify flow regime. The axes are superficial momentum fluxes which calculate by product of phase density and the square of the superficial velocity (volumetric flow rate over the tube cross-section area). This map is useful in all water and air system over a range of pressures in small diameters. The drawback of this map is when in heated tube, it is impossible to know true content of the particular phase and it also has some uncertainty near regime boundary because of the precision of calculation. So this method could be only used as a general guide rather an exact indication.

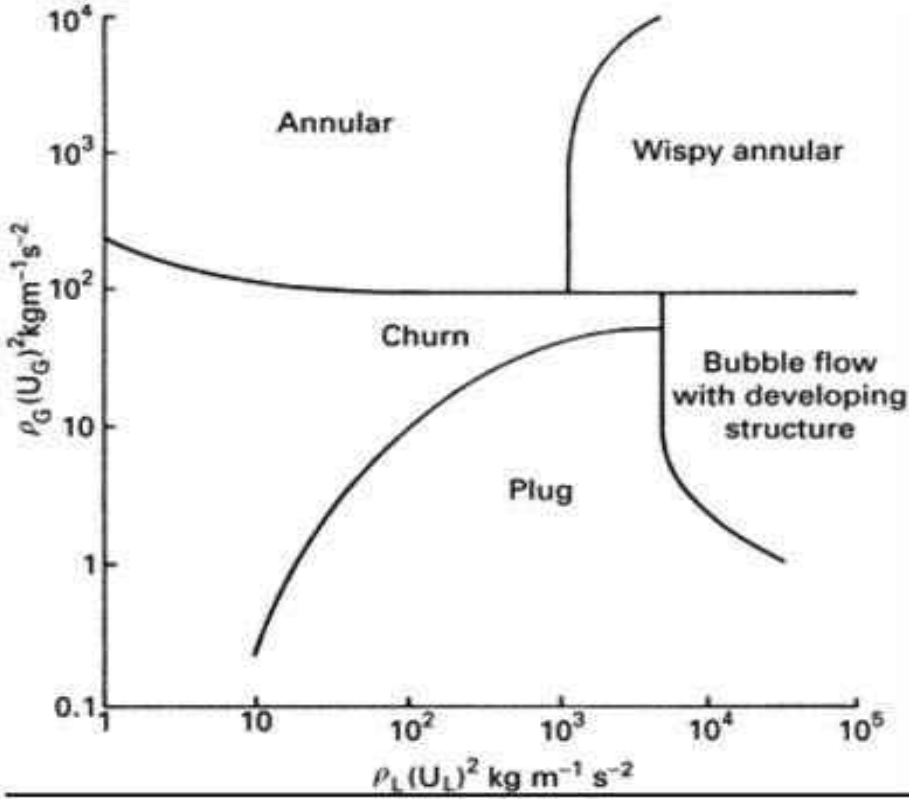


Figure 1 Flow regime map (Hewitt and Robert's (1969)) **[5]**

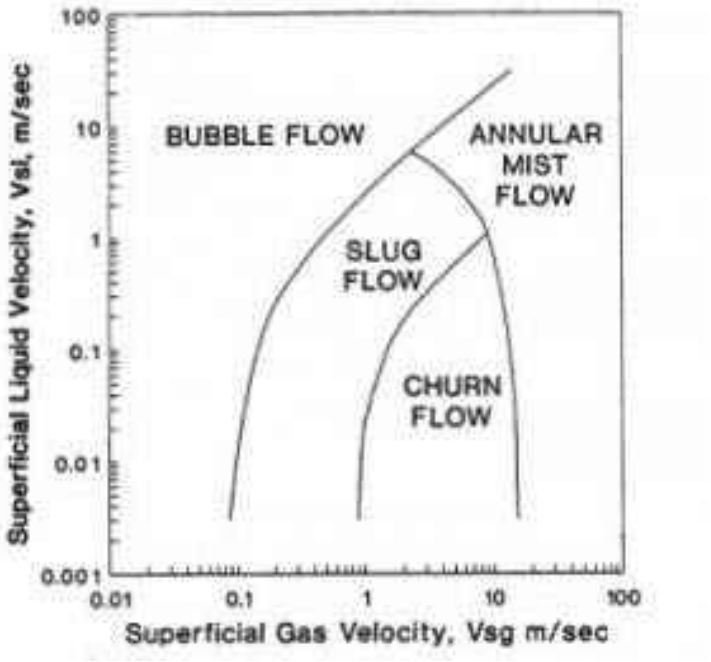


Figure 2 Vertical Flow regime map of Dukler and Taitel [6]

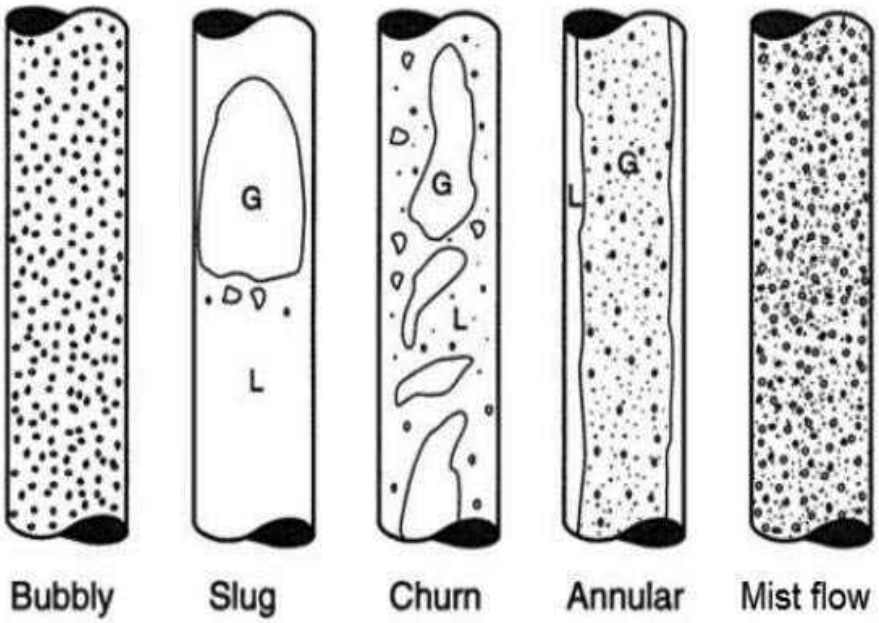


Figure 3 Flow Pattern in Vertical Upwards Flow (Weisman, J. Two-phase flow patterns) [7]

- Bubble flow: In two-phase flow, when there are a lot of small bubbles dispersed in a continuum of liquid, the deformable bubbles keep moving and complex interactions take place between liquid and bubbles.
- Slug flow: Slug flow sometimes also is called plug flow. With the bubbles moving upwards to a certain height, bubble agglomeration and coalescence happened. Once the bubbles diameter is the same with the tube inner-diameter the large bubbles will separate the liquids. The bubbles shaped like a bullet we call it Taylor bubble, when these bubbles appear it means reaching the boundary between bubble flow and slug flow. The slug could cause pressure oscillation and result in serious problem in the production system of oilfield, so slug catcher is always installed to maintain system stability before the oil flows into the separator.
- Churn flow: In large dimeters tube, when the velocity of gas flow increases, these Taylor bubbles will twist and break to form an unstable regime in the tube, both liquid phase and gas phase would be unstable. However, in a small diameters tube, the oscillation will not take place and we could observe a smoother transition from slug flow to churn flow.
- Annular flow: If the gas flow velocity becomes higher the liquid phase will flow along with the wall of the tube which like a thin film. And the gas phase will flow in the center of the tube. At the same time, there are also some liquid drops contained in the gas phase.

- Mist flow: With higher flow rates and very high flow velocity, all the liquids becomes droplets in the gas core of annular flow. At this time, we call this flow regime as mist flow.

**Flow pattern definition for horizontal flow**

For horizontal flows, the classical flow regime map was proposed by Baker. This map is a series plots against superficial liquid and gas mass flow rate and then this chart was modified by Scott (1963) and Schicht(1969) to have a more accurate result.

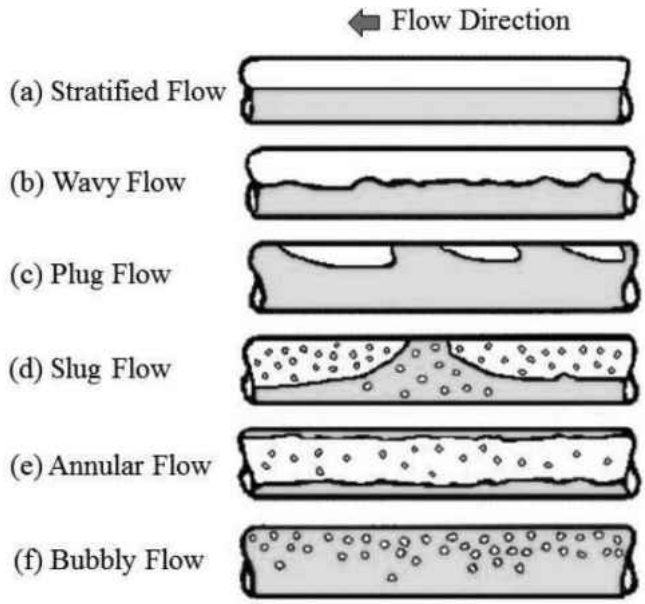


Figure 4 Flow Pattern in horizontal Flow (Conference: ASME 2017 International Mechanical Engineering Congress and Exposition) [8]

- Stratified flow: Liquid flows at the bottom of the tube and gas flows along the top.
- Wavy flow: With gas velocity gets higher in stratified flow, waves form at the boundary of two phase, resulting in more friction.
- Plug flow: The character of this flow regime is bullet-shaped bubbles formed and moving close to the top of the tube.

- Slug flow: When the wave is big enough to touch the top of the tube, becoming closer to the gas pass and causing the pressure sudden change when this path closed. It is the beginning of the slug flow pattern.
- Annular flow: This flow regime formed in a high gas flow rate, liquid droplet is in the core of the gas phase. And because of the influence of the gravity the film at the bottom is thicker than the top film.
- Bubbly flow: Bubbles are dispersed in the cross section. When the gas flow rate is low, bubbles tend to flow at the top of the tube and becoming foam in a high rate.

**Obtaining flow pattern information**

The flow pattern is always distinguished by the observation of the flow. There are several technologies used to identify the necessary parameters.

Firstly, to distinguish flow-pattern, visualization technique given by Hewitt and Hall Taylor (1970) [9]should be applied. High speed photography should be used for high velocity flow. However, because of complex light refraction the image we get is difficult to interpret. Generally, this problem causes people to search for a more accurate method to find out flow pattern. With the help of X-ray which only depends on absorption, people could obtain meaningful picture to interpret the fluid regime.

Then Lopina and Friori (1967) [10]and Bergles (1969) [11] found a new method which used a conductance probe to measure the conductance between tip and tube wall. Unfortunately, the contact between needles may influence the quantity of the result.

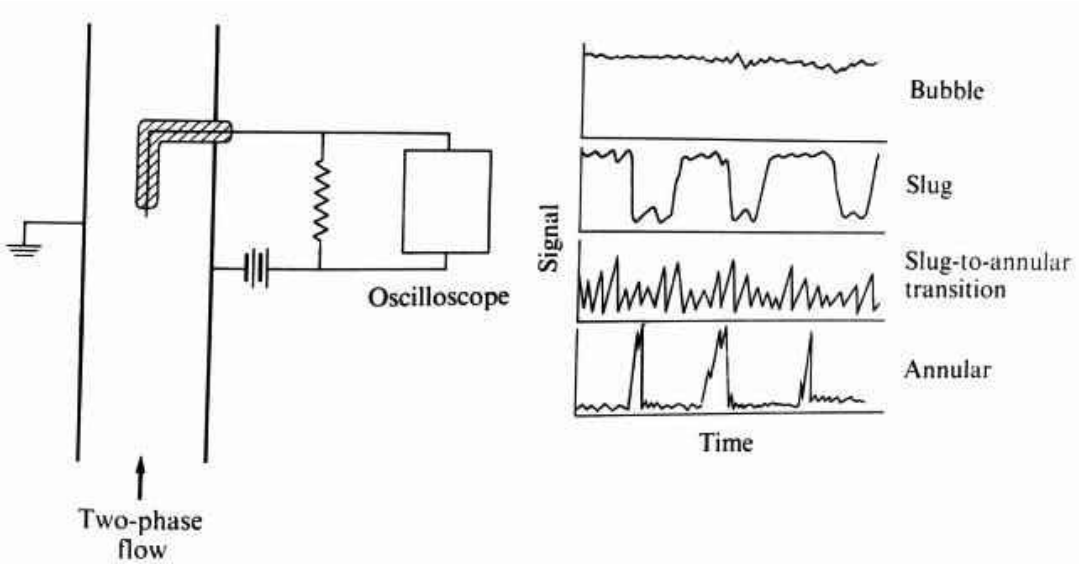


Figure 5 Conductance-probe technique for evaluation of flow pattern in two-phase flow (Bergles.1969) [11]

Jones and Zuber (1974) developed another technique using high-intensity X-ray beam through the flow to get the instantaneous void fraction with a detector. With the function of time bubble flow's density peak appears at a low fraction, for slug flow it will have two peaks, for annular flow the peak appears at a high void fraction. [12]

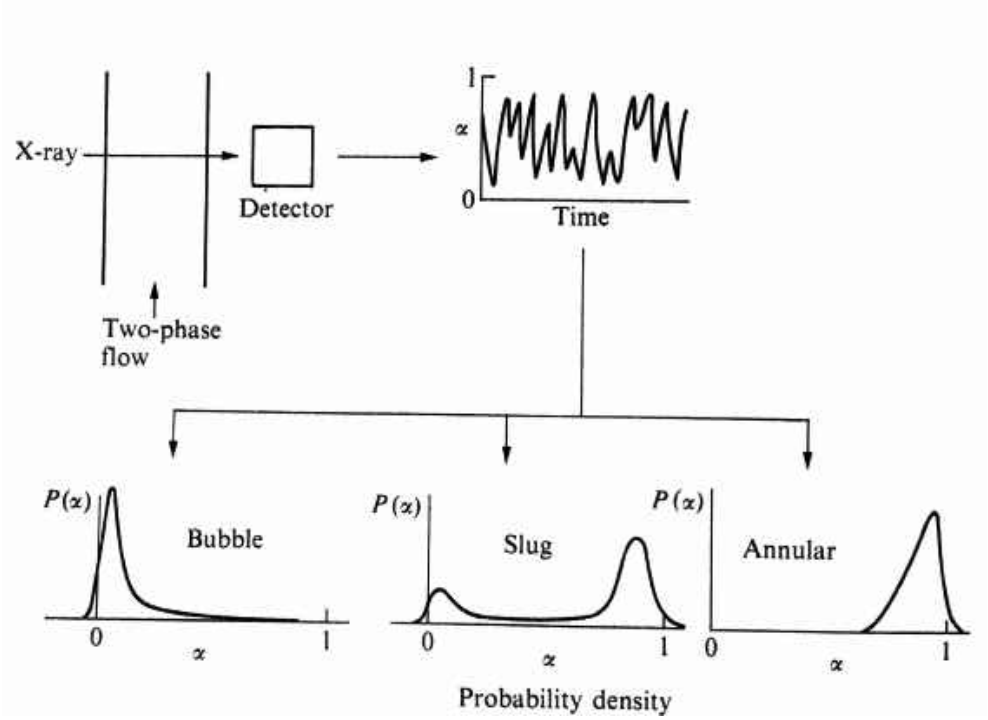


Figure 6 X-ray absorption technique for determination of flow pattern (Jones and Zuber 1974) [12]

**Methods to detect Void fraction**

Void fraction is the fraction of volume occupied by gas phase. In two-phase flow regime, this parameter plays an important role to distinguish different flow patterns, and help us know the interfacial transport of the fluid, also effect pressure drop and heat transfer. Many scholars had developed a lot of methods to measure it.

$$\alpha = \frac{A_G}{A} \tag{1.13}$$

$$1 - \alpha = \frac{A_L}{A} \tag{1.14}$$

Mass velocities of gas and liquid phase:

$$\text{Gas phase} \qquad G_g = \rho_g u_g \alpha \tag{1.15}$$

$$\text{Liquid phase} \quad G_l = \rho_l u_l (1 - \alpha) \tag{1.16}$$

Average density of the two-phase

$$\rho = (1 - \alpha)\rho_l + \alpha\rho_g \tag{1.17}$$

**Side-tube method**

This method considered about the gravitational pressure loss and neglect the frictional pressure lose, acceleration pressure loss. In the experiment, they use 3.81 cm and 5.08 cm diameters pipe and water and gas velocities are 0.01 m/s and 0.5 m/s respectively. The accuracy of the equation they found would be influenced by frictional force and minor losses (flow, pressure, or energy reduction in piping system) in pipe flow. [13]

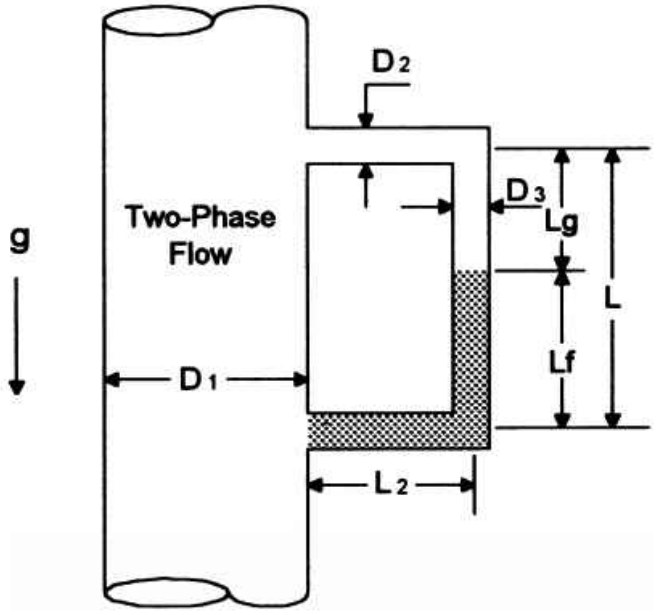


Figure 7 Void fraction measurement by using the side-tube method [13]

$$\alpha_3 = \frac{L_g}{L_g + L_f} = \alpha_1 \tag{1.18}$$

where

$\alpha_3$: Void fraction in side tube

$\alpha_1$ : Void fraction in test tube

$L_g + L_f$: length of side-tube in vertical

$L_g$ : length of the gas phase

**Image analysis technique**

Ugandhar Puli, A.K. Rajvanshi (2012) [14] have tried to analyze the void fraction using a high speed camera and processing image by the software. Tomio Okawa (2006) [15] also use this measure to test the void fraction and test the influence by four parameters: nucleation site density (total number of nucleation sites diving by the total heated area) [16], bubble release frequency, bubble lifetime and bubble size.

With the help of this method, we could get a reliable result and determine the void fraction even without the information about the fluid and fluid flow conditions.

**Conductivity probe methods**

The principle of this method is getting local time-averaged interfacial area concentration. And record the time interval of an interface pass a local point. Kim S [17] used four-sensor conductivity probe in case the bubbles' shapes significantly vary such as bullet shape, and cap. This method could get three interfacial velocities from one point and will not limited by the bubbles shape. The limitation of this method is caused by the size of probe, it results in more bubbles missing the probe.

There are also some other equations developed by scholars which is well-known to calculate void fraction.

| | |
|---|---|
| **Homogenous Model** | $\alpha = \left[1 + \frac{1-x}{x}\left(\frac{\rho_v}{\rho_l}\right)\right]^{-1}$ |
| **Baroczy (1965)** | $\alpha = \left[1 + \left(\frac{1-x}{x}\right)^{0.74}\left(\frac{\rho_v}{\rho_l}\right)^{0.65}\left(\frac{\mu_l}{\mu_v}\right)^{0.13}\right]^{-1}$ |
| **Zivi (1964)** | $\alpha = \left[1 + \frac{1-x}{x}\left(\frac{\rho_v}{\rho_l}\right)^{2/3}\right]^{-1}$ |
| **Lockhart and Martinelli (1949)** | $\alpha = \left[1 + 0.28\left(\frac{1-x}{x}\right)^{0.64}\left(\frac{\rho_v}{\rho_l}\right)^{0.36}\left(\frac{\mu_l}{\mu_v}\right)^{0.07}\right]^{-1}$ |
| **Thom (1949)** | $\alpha = \left[1 + \left(\frac{1-x}{x}\right)\left(\frac{\rho_v}{\rho_l}\right)^{0.89}\left(\frac{\mu_l}{\mu_v}\right)^{0.18}\right]^{-1}$ |
| **Steiner (1993)** | $\alpha = \frac{x}{\rho_v}\left([1 + 0.12(1-x)]\left[\frac{x}{\rho_v} + \frac{1-x}{\rho_l}\right] + \frac{1.18(1-x)\left[g \times \sigma(\rho_l - \rho_v)\right]^{0.25}}{G \times \rho_l^{0.5}}\right)^{-1}$ |
| **El Hajal et al. (2003)** | $\alpha = \frac{\alpha_h - \alpha_{Steiner}}{\ln\left(\frac{\alpha_h}{\alpha_{Steiner}}\right)}$ |
| **Smith (1969)** | $\alpha = \left\{1 + \left(\frac{\rho_v}{\rho_l}\right)\left(\frac{1-x}{x}\right) \times \left[K + (1-K)\sqrt{\frac{\left(\frac{\rho_l}{\rho_v}\right) + K\left(\frac{1-x}{x}\right)}{1 + K\left(\frac{1-x}{x}\right)}}\right]\right\}^{-1}$ |
| **Premoli et al. (1971)** | $\alpha = \frac{x}{x + S(1-x)\,\rho_v/\rho_l}$ |
| **Yashar et al. (2001)** | $\alpha = \left[1 + \frac{1}{Ft} + X_{tt}\right]^{-0.321}$ |

Figure 8 Well-known void fraction correlations (Burak dibek, Hakan demir, determination of void fraction by image processing) [18]

Liquid Superficial Velocity

$$u_L = \frac{V_L}{1-\alpha} \tag{1.19}$$

Gas Superficial Velocity

$$u_G = \frac{V_G}{\alpha} \tag{1.20}$$

Total Superficial Velocity

$$V = V_L + V_G \tag{1.21}$$

$V_L$: Superficial velocity of liquid

$V_G$: Superficial velocity of gas

$u_L$: Liquid velocity

$u_G$: Gas velocity

$\alpha$: Void fraction

Slip ratio

$$K = \frac{u_G}{u_L} = \left(\frac{x}{1-x}\right)\left(\frac{1-\alpha}{\alpha}\right)\frac{\rho_L}{\rho_G} \tag{1.22}$$

Slip velocity

$$u_{slip} = u_G - u_L \tag{1.23}$$

# CHAPTER 2

## II. PRESSURE DROP ANALYSIS IN VERTICAL PIPELINE

Measuring the pressure change in borehole is useful to predict the production and makes it easier to design the downstream equipment such as separator or electric dehydrator.

The pressure change in the vertical tube is a summation of three factors: friction and liquid-gas interface, gravity, and acceleration changing. Average void fraction is widely used to predict the gravitation pressure gradient terms. The acceleration term is negligible in homogeneous flow model.

Scholars had already done a large amount of experiments on friction because it was one of the important reasons contributing to total pressure-drop. There are two models to calculate friction: one is a homogeneous flow model and another is a separated flow model. Some of the approaches are introduced

like Lockhart-Martinelli approach (1949) [19], and Muller-Steinhagen and Heck correlation (1986) [20]. With literature review, the existing databases for vertical upward flow always use the tube diameter of nearly 25mm and the superficial liquid velocity is nearly 4m/s. I choose to use larger diameters tube to have a comparison. The water and air flow velocities range from 0.01 to 20 m/s and 0.05 to 10 m/s, separately. With different combination of these two phases we could get all kinds of flow regimes described by Govier and Aziz (1972) [21], Hewitt (1969) [22], Delhaye (1994) [23].

Two phase flow pressure drop is dominated by friction, acceleration and gravity.

$$\Delta \boldsymbol{P} = \Delta \boldsymbol{P}_{\boldsymbol{friction}} + \Delta \boldsymbol{P}_{\boldsymbol{acceleration}} + \Delta \boldsymbol{P}_{gravity} \quad (2.1)$$

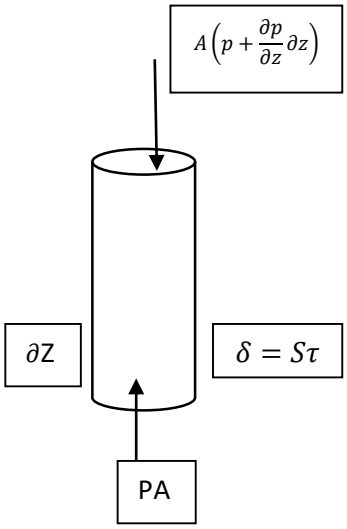


Figure 9 Force balance on element of pipe

**Single phase**

Single-phase pipe flow in vertical pipe, fluid gravity, and friction between the tubing wall and fluid acceleration will cause the pressure drop. For the steady flow in horizontal pipe, the gravity term of the pressure gradient is zero because of no change in the elevation and the acceleration part is also negligible.

*Momentum balance*

$$\int_A \left\{p - \left(p + \frac{\partial p}{\partial z}\partial z\right)\right\} dA = \int_S \tau\, \partial z ds + \int_A \frac{\partial}{\partial z}(Gu)\partial z \partial A + \int_A \rho g \partial z \partial A \quad (2.2)$$

Pressure force | Frictional force | Momentum change force | Weight force

In **Eq. 2.2,** P is the pressure, $\boldsymbol{\tau}$ is the shear stress of the tube, G is $\rho u$. Because the continuity of mass, G will not change along the channel.

After Rearranging

$$-\frac{\partial p}{\partial z} = \frac{S}{A}\tau + G\frac{du}{dz} + \rho g \tag{2.3}$$

*Energy balance*

$$d(pv) + dU + d\left(\frac{1}{2}u^2\right) + d(gz) = dp - dw \tag{2.4}$$

$$dU = dp + dF - pdv \tag{2.5}$$

V: the fluid specific volume

$$-\frac{\partial p}{\partial z} = \rho\frac{dF}{dz} + G\frac{du}{dz} + \rho g \tag{2.6}$$

dF: friction loss

From 2.3 and 2.6 we know that:

$$\frac{S}{A}\tau = \rho\frac{dF}{dz} \tag{2.7}$$

**Two-phase flow**

Fluid behavior in multiphase flow is more complex than the single-phase flow, because the different density and different superficial velocity within the phases may separate with each other. Different velocities in the pipe could form all kinds of flow patterns we discussed before.

So, understanding the basic definitions of flow regimes as well as the calculations of all the flow parameters like void fraction, pressure drop, and fluid velocities play an important role in solving multiphase flow problems.

Two-phase flow momentum and energy balances give:

$$-\frac{\partial p}{\partial z} = \frac{S}{A}\tau + \frac{d}{dz}[\alpha G_G u_G + (1-\alpha)G_L u_L] + g(\alpha\rho_G + (1-\alpha)\rho_L) \tag{2.8}$$

In this equation, we need to know the wall shear stress ($\tau$), surface area (S), and cross-sectional area (A) to calculate the frictional part which would be mentioned later and obtain the void fraction ($\alpha$) with the methods we talked before to determine the pressure gradient. In high flow rate conditions, friction is one of the contributors to the pressure loss. On the other hand, the frictional part also depends on different flow pattern in the pipe.

**Wall shear stress**

Wall shear stress is the shear stress in the layer of fluid next to the wall of the tube. The most well-known method to define wall shear stress is consistent that with single-phase studies.

$$\tau_{wg} = \frac{1}{2} f_g \rho_g u_g^2 \tag{2.9}$$

$$\tau_{wl} = \frac{1}{2} f_l \rho_l u_l^2 \tag{2.10}$$

$$\tau_{wi} = \frac{1}{2} f_i \rho_g (u_g - u_l)^2 \tag{2.11}$$

where:

$f_l$: Liquid friction factor

$f_g$: Gas friction factor

$f_i$: Interfacial friction factor

$$f_k = C Re_k^m \tag{2.10}$$

$k$ indicate different phase for laminar flow $C = 16$ and $m = -1$ is widely used, for turbulent flow in smooth tubes $C = 0.046$ and $m = -0.2$ is widely used. When the fluid

flow is between laminar and turbulent flow, friction factor can be calculated with the equation $f = (f_{lam}^3 - f_{turb}^3)^{1/3}$, which could eliminate the discontinuity in the transition. where:

Re: Reynolds number given by

$$Re = \frac{\rho u D_H}{\mu} \tag{2.11}$$

$D_H$: the hydraulic diameter of the tube

$\rho$ : the density of the fluid

$u$: the mean velocity of the fluid

$\mu$ : the dynamic viscosity of the fluid

**Models for Pressure drop prediction**

For the two-phase frictional pressure drop modeling approaches, many scholars have developed several methods for it. Among all these methods we could divided it into two categories: Homogeneous flow model and Separated flow model.

**Homogeneous flow model**

It is always defined as the gas phase superficial velocity is equal to liquid phase superficial velocity. Then the mixture will have a certain density and mean properties, it is the simplest way to solve some problems.

The fraction factor in homogeneous flow is a function of the Reynolds number:

$$f_m = 0.079 Re_m^{-0.25} \tag{2.12}$$

Reynolds number is defined as:

$$Re = \rho u d / \mu \tag{2.13}$$

Different with **Eq. 2.11**

$\mu$ is the mixture viscosity

There are some well-known equations to calculate mixture viscosity.

McAdams et al. (1942) [24] $1/\mu = x/\mu_g + (1-x)/\mu_l$ (2.14)

Dukler et al. (1964) [25] $\mu = \alpha\mu_g + (1-\alpha)\mu_l$ (2.15)

Beattie and Whalley (1982) [26] $\mu = \alpha\mu_g + (1-\alpha)(1+2.5\alpha)\mu_l$ (2.16)

**Separated flow model**

- Lockhart-Martinelli approach

Lockhart and Martinelli (1949) [19] developed a two-phase flow pressure drop model. They defined a parameter $\emptyset_f^2$(frictional multiplier) as a function of Martinelli parameter (X):

Liquid phase frictional multiplier: $\emptyset_l^2 = \frac{dP_f/dz}{dp_{f,L}/dz}$ (2.16)

Gas phase frictional mulipluer: $\emptyset_G^2 = \frac{dP_f/dz}{dp_{f,G}/dz}$ (2.17)

$dP_f/dz$ indicate the pressure gradient caused by friction. So $dp_{f,L}/dz$, $dp_{f,G}/dz$ represent the liquid and gas phase flow pressure gradient in the pipe, respectively. And the Martinelli parameter (X) is defined as:

$$\boldsymbol{X^2} \equiv \frac{dp_{f,L}/dz}{dp_{f,G}/dz} \quad (2.18)$$

- Müller-Steinhagen and Heck (1986) [20] approach

The frictional pressure drop in two-phase fluid flow is basically known as an empirical interpolation and the correlation can also be used under single-phase flow conditions.

The Müller-Steinhagen and Heck (1986) correlation is given as follows:

$$\left(\frac{dp}{dL}\right)_{f,tp} = \beta(1-x)^{1/C_{MS}} + Bx^{C_{MS}} \tag{2.19}$$

where $C_{MS}$ is 3 and $\beta$ is given by

$$\beta = A + 2(B-A)x \tag{2.20}$$

$$\left(\frac{dp}{dL}\right)_{f,L} = f_L \frac{2G^2}{\rho_L d_h} = A \tag{2.21}$$

$$\left(\frac{dp}{dL}\right)_{f,V} = f_V \frac{2G^2}{\rho_V d_h} = B \tag{2.22}$$

$$\begin{cases} f_L = \frac{16}{Re_L},\ f_V = \frac{16}{Re_V} & \text{for} \quad Re_L, Re_V \leq 1187 \\ f_L = \frac{0.079}{{Re_L}^{1/4}},\ f_V = \frac{0.079}{{Re_V}^{1/4}} & \text{for} \quad Re_L, Re_V > 1187 \end{cases}$$

$$Re_L = \frac{G d_h}{\mu_L},\ Re_V = \frac{G d_h}{\mu_V}$$

# CHAPTER 3

# III. APPLICATION OF PRESSURE DROP ANALYSIS

In this section we designed a new model to evaluate polished rod load of sucker rod pumping system. Sucker rod pumps provide mechanical energy to lift oil from bottom hole to surface when oil wells do not have enough energy to produce the oil through natural flow. It is efficient, simple, easy to be operated, and can be applied to slim holes, multiple completions, and high-temperature and viscous oils. The disadvantages include excessive friction in crooked holes, solid-sensitive problems, low efficiency in gassy wells, limited depth, and bulky volume. The load on the rod is one of the key factors that dictate the maintenance frequency of pumping unit, energy consumed to lift the fluid, and the optimization of pumping system operating parameters. The cyclic load applied on the rod causes the fatigue and finally the failure of the rod if not designed properly. The rod load is a function of friction force, plunger acceleration/deceleration, weights of plunger, fluid being lifted, and sucker rods string, and the pressures above and below on plunger. Literature review indicates that a model to accurately calculate the load of a pumping cycle is highly desired. In this study, we couple the wellbore with reservoir performance to better analyze the dynamics of pump system, which yields more accurate results.

Force balance during the pumping cycle is analyzed. Friction force due to the movement of the plunger and the rod, buoyant force, and gravity force are included in the

modeling. The effects of acceleration and deceleration of the plunger on rod are considered. The sensitivity of pumping speed is investigated. This study proposed a more general model comparing with former researches because more factors that affect the load applying on rod are included. Including the friction force due to the viscous fluid is critical to rod load analysis in pumping heavy oil.

**Polished Rod Load Analysis**

A complete pumping circle consists of upstroke and down-stroke. Polished rod or sucker rod is subject to various load in one pumping circle. Forces acting on the polished rod change during the upstroke and down-stroke are analyzed separately in this study. Basically, forces acting at any given point in sucker rod can be analyzed using similar principle. It is noted that the phase of fluid affects the polished rod load. In this research, we consider single-phase liquid well. Loads in the upstroke and down-stroke are calculated separately.

**In single-phase liquid well**

As shown in **Fig. 9**, during the upstroke, traveling valve is close while standing valve is open. For single phase oil production, during the upstroke forces acting on the polished rod include

- Pressure beneath plunger acting on the cross-section area of the plunger
- Weight of fluid column above plunger acting on the cross-section area of the plunger
- The drag force caused by liquid slippage downward past the plunger (oil slips along the annulus between plunger and working barrel when plunger travels upward.) or friction of the plunger when contacting the working barrel. Because we assume

plunger does not touch the working barrel, the friction force on the plunger is caused by fluid-plunger friction.

- Weight of the plunger
- Weight of the sucker rod
- Friction of the fluid with the tubing
- Acceleration of sucker rod
- Surface pressure (line pressure and restrictions) acting against the plunger during the upstroke
- The upward flow velocity of fluid above plunger is almost the same as that of plunger/sucker rod string. Therefore, the frictional force between fluid and sucker rod string is negligible.

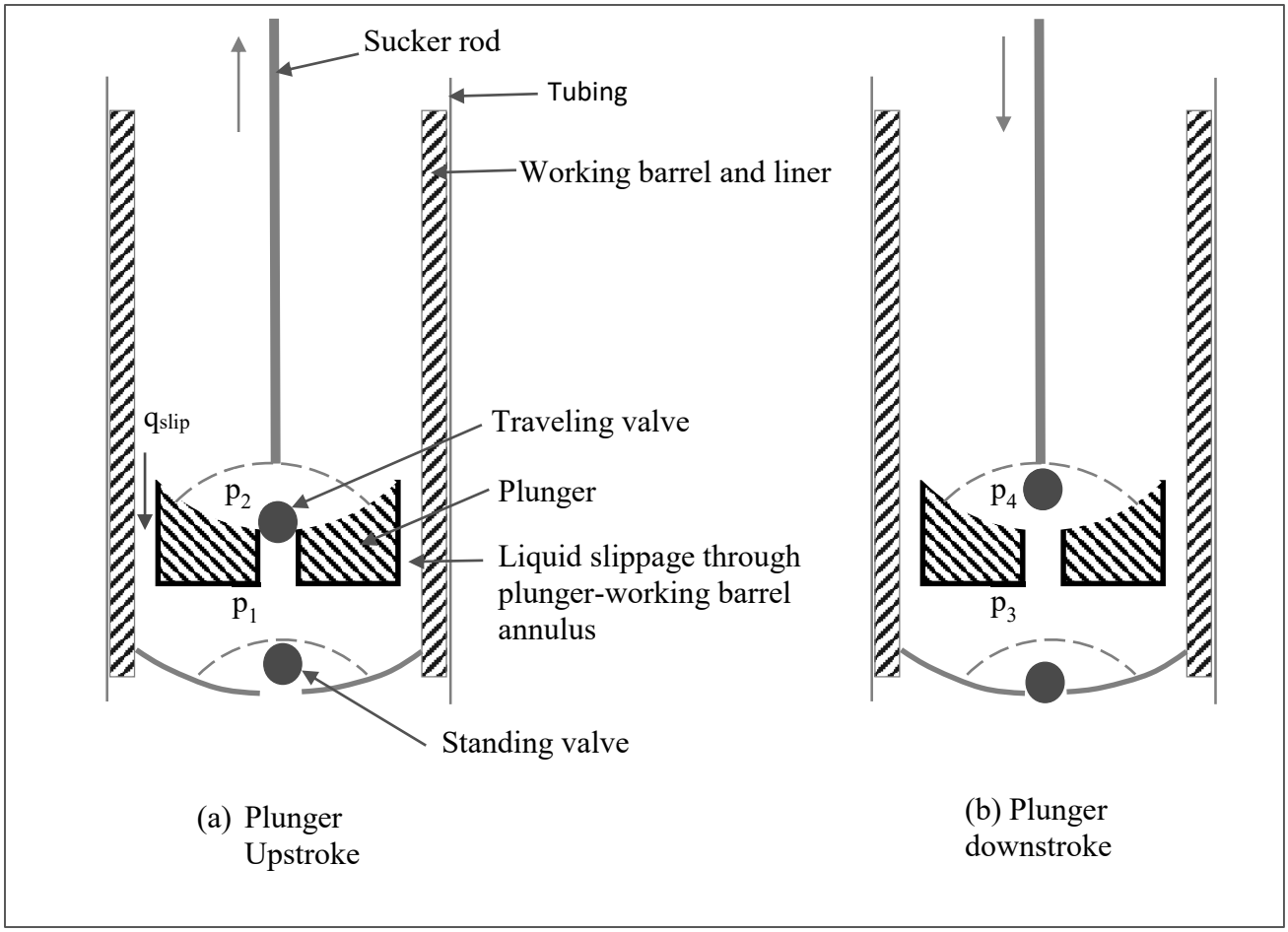


Figure 10 Downhole components of a sucker rod pump and the movement of standing and traveling valves

Force balance in the vertical direction gives

$$F_{PR} = W_f + W_p + W_r + F_{\text{drag, tubing-fluid}} + F_{\text{drag, plunger-fluid}} + F_{\text{acceleration}} + p_{wh}A_{plunger} - p_1 A_{plunger} \quad \text{.....(3.1)}$$

where

$A_{plunger}$ = cross-sectional area of plunger

$F_{\text{acceleration}}$ = force needed to accelerate sucker rod

$F_{\text{drag, plunger-fluid}}$ = drag force acting on plunger caused by liquid slippage through plunger-working barrel annulus

$F_{\text{drag, tubing-fluid}}$ = frictional force between fluid and tubing

$F_{PR}$ = polished rod load

$p_1$ = pressure beneath plunger

$p_{wh}$ = flowing wellhead pressure

$W_f$ = weight of fluid column above plunger

$W_p$ = weight of plunger

$W_r$ = weight of sucker rod string.

**Weights of fluid, plunger, and rod**

Weight of fluid column above plunger can be calculated by

$$W_f = \frac{g}{g_c}\rho_f L_{rod}\left(A_{plunger} - A_{rod}\right) \quad (3.2)$$

Weight of sucker rod can be calculated by

$$W_r = \frac{g}{g_c}\rho_r L_{rod} A_{rod} \quad (3.3)$$

where

$A_{rod}$ = cross-sectional area of sucker rod

$L_{rod}$ = length of sucker rod, which is equal to depth to plunger

$g_c$ = constant for unit conversion

$g$ = gravitational acceleration

$\rho_f$ = fluid density

$\rho_r$= sucker rod density.

**Drag force between tubing-fluid and sucker rod-fluid**

The drag forces of the liquid applying on the tubing and sucker rod are the frictional force caused by tubing wall and sucker rod wall when plunger travels upward as shown in **Fig. 9**. Because the fluid moves almost at the same velocity as sucker rod. The friction force is

negligible between sucker rod and fluid. The frictional pressure drop across the tubing-sucker rod annulus is caused by frictional force between tubing and fluid. Following assumptions are made in the frictional force calculation:

1) The flow in annulus is steady-state flow.
2) Sucker rod is moving in the center of tubing and does not touch the tubing wall.
3) The fluid is Newtonian.
4) Fluid viscosity and density are constant.

When the sucker rod (and plunger) moves with a velocity, $v_{rod} = v_{plunger}$, part of fluid displaced by plunger flow through wellhead to surface and the rest slips back to working barrel. The slippage of fluid results in the drag force on the flank of plunger. According to the force equilibrium, we have the following form.

$$p_{wh} + \rho_f \frac{g}{g_c} L_{rod} + \Delta p_{f\_production} = p_2 \quad \text{..... (3.4)}$$

where

$P_2$= pressure above plunger

$\Delta p_{f\_production}$= frictional pressure-drop for fluid production.

The frictional pressure drop is balanced by the drag force between fluid and tubing wall. The calculation of frictional pressure drop depends on the flow regimes: laminar and turbulent. When Reynolds number is less than 2100, flow can be considered as laminar; otherwise, it is turbulent.

### 3.3.1 Laminar flow

When plunger moves at a velocity, $v_{plunger}$, the volume of the fluid displaced by the plunger is equal to sum of fluid volume flow through wellhead (or production) and slippage volume.

$$V_{displaced\ by\ plunger} = V_{production} + V_{slip\_upstroke} \quad \text{..... (3.5)}$$

Expressing in rate we have

$$q_{displaced\ by\ plunger} = q_{production} + q_{slip\_upstroke} \quad \text{..... (3.6)}$$

where

$V_{diaplaced\ by\ plunger}$ = fluid volume displaced by plunger

$V_{production}$ = fluid volume flow through wellhead

$V_{slip\_upstroke}$ = slippage volume during upstroke

$q_{diaplaced\ by\ plunger}$ = rate of fluid volume displaced by plunger

$q_{production}$ = production rate

$q_{slip\_upstroke}$ = slippage rate in upstroke.

Now we calculate the frictional pressure drop for fluid production. It is reasonable to use plunger velocity to approximate sucker rod and polished rod velocities. When fluid is lifted by the plunger, sucker rod velocity is almost the same as fluid velocity at the sucker rod wall. The frictional pressure drop is caused by the drag force between fluid and tubing wall. The annulus between sucker rod and tubing can be represented by **Fig. 10(a)**

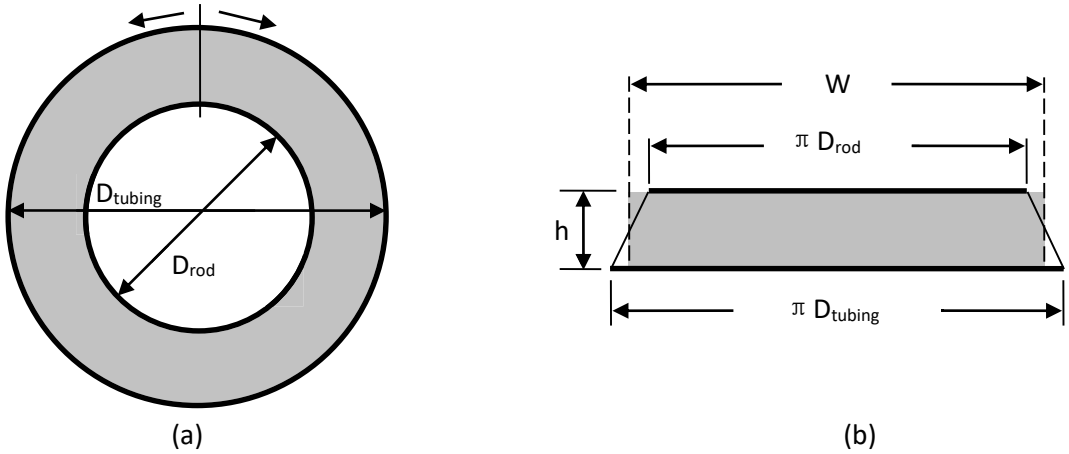


Figure 11 Representing the annulus as a slot: (a) annulus and (b) equivalent slot

For the case of laminar flow, we assume fluid velocities on tubing wall is zero and reach maximum on the wall of sucker rod. Now we consider a control fluid volume in the annulus, which can be represented by rectangular slot flow as far as the ratio of sucker rod diameter to tubing diameter exceeds 0.3 (**Fig. 10 (b)**). Now consider a rectangular slot with an area of A and height of h used to represent the annular flow (**Fig. 11**). The area and height can be expressed in diameters, which are

$$A = Wh = \frac{\pi}{4}\left(D_{tubing}^2 - D_{rod}^2\right) \quad (3.7)$$

where

$$W = \frac{\pi}{2}\left(D_{tubing} + D_{rod}\right) \quad (3.8)$$

and

$$h = \frac{1}{2}\left(D_{tubing} - D_{rod}\right) \quad (3.9)$$

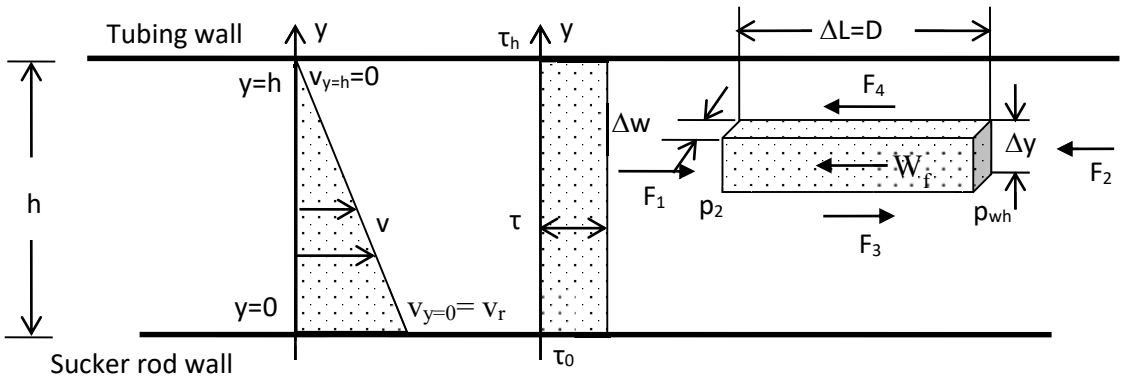


Figure 12 Free body diagram for a controlled fluid volume in a slot representing sucker rod-tubing annulus

We deal with a controlled fluid volume (**Fig. 11**) with width *Δw* and thickness *Δy*. Force equilibrium in vertical direction gives

$$F_1 + F_3 = F_2 + F_4 + W_f \ldots\ldots (3.10)$$

where

$$F_1 = p_2 \Delta w \Delta y = p_{wh} \Delta w \Delta y + \frac{dp_f}{dL} \Delta L \Delta w \Delta y + \rho_f \frac{g}{g_c} \Delta L \Delta w \Delta y = \left(p_{wh} + \frac{dp_f}{dL} L_{rod} + \rho_f \frac{g}{g_c} L_{rod}\right) \Delta w \Delta y \quad (3.11)$$

$$F_2 = p_{wh} \Delta w \Delta y \ldots\ldots (3.12)$$

$$F_3 = \tau_y \Delta w \Delta L = \tau_y \Delta w L_{rod} \ldots\ldots (3.13)$$

$$F_4 = \tau_{y+\Delta y} \Delta w \Delta L = \left(\tau_y + \frac{d\tau}{dy} \Delta y\right) \Delta w L_{rod} \ldots\ldots (3.14)$$

and

$$W_f = \rho_f \frac{g}{g_c} L_{rod} \Delta w \Delta y \ldots \quad (3.15)$$

where

$\Delta L$ = length of controlled fluid volume, for fluid above plunger, length of fluid column is same as sucker rod length, or the depth to plunger, $\Delta L = L_{rod}$

$D_{rod}$ = rod diameter

$D_{tubing}$ = tubing diameter

$\tau$ = shear stress

$\frac{dp_f}{dL}$ = frictional pressure gradient in annulus

$\frac{d\tau}{dy}$ = shear stress gradient in $y$ direction

Substituting **Eqs. 3.11** through **3.15** into **Eq.3.10** yields

$$\left(p_{wh} + \frac{dp_f}{dL} L_{rod} + \rho_f \frac{g}{g_c} L_{rod}\right) \Delta w \Delta y + \tau_y \Delta w L_{rod} = p_{wh} \Delta w \Delta y + \left(\tau_y + \frac{d\tau}{dy} \Delta y\right) \Delta w L_{rod} + \rho_f \frac{g}{g_c} L_{rod} \Delta w \Delta y \ldots \quad (3.16)$$

Expanding and canceling out the same terms on both sides gives

$$\frac{dp_f}{dL} L_{rod} \Delta w \Delta y = \frac{d\tau}{dy} \Delta y \Delta w L_{rod} \ldots \quad (3.17)$$

Dividing **Eq.3 17** by $L_{rod} \Delta w \Delta y$, we have

$$\frac{dp_f}{dL} = \frac{d\tau}{dy} \ldots \quad (3.18)$$

Because d$p_f$/d$L$ is not a function of $y$, and $\tau$is constant in y-direction. **Eq. 18** can be expressed in

$$\Delta p_{f\_production}\left[\frac{\pi}{4}\left(D_{tubing}^2 - D_{rod}^2\right)\right] = \pi D_{tubing} L_{rod}\tau \text{..} \quad (3.19)$$

Shear stress is a function of viscosity and shear rate

$$\tau = \mu\dot{\gamma} = -\mu\frac{dv}{dy} \text{..} \quad (3.20)$$

where shear rate, $\dot{\gamma}$, is

$$\dot{\gamma} = -\frac{dv}{dy} \text{..} \quad (3.21)$$

where

$\mu$ = fluid viscosity

$v$ = fluid velocity.

**Eq.3.19** becomes

$$\Delta p_{f\_production} = \frac{-\pi D_{tubing} L_{rod}}{\frac{\pi}{4}\left(D_{tubing}^2 - D_{rod}^2\right)}\left(\mu\frac{dv}{dy}\right)$$

or

$$dy = -\frac{4 D_{tubing} L_{rod}\mu}{\Delta p_{f\_production}\left(D_{tubing}^2 - D_{rod}^2\right)} dv \text{..} \quad (3.22)$$

The flow rate $q$ is the product of velocity $v$ and area $A$. Integrating the control volume flow velocity throughout the interval from 0 to $h$ we obtain total flow rate

$$q_{production} = \int v dA = \int_0^h vW dy \quad (3.23)$$

Substituting **Eq. 3.22** into **3.23** gives

$$q_{production} = \int_0^h v\left[\frac{\pi}{2}\left(D_{tubing} + D_{rod}\right)\right]\left[-\frac{4D_{tubing}L_{rod}\mu}{\Delta p_{f\_production}\left(D_{tubing}^2 - D_{rod}^2\right)}\right]dv \quad (3.24)$$

Integrating **Eq. 3.24** we have

$$q_{production} = \frac{\pi D_{tubing}L_{rod}\mu v^2}{\Delta p_{f\_production}\left(D_{tubing} - D_{rod}\right)}\Bigg|_{v \text{ at } y=h}^{v \text{ at } y=0} \quad (3.25)$$

Applying the boundary conditions

$$v = v_{rod} \text{ at } y = 0 \quad (3.26)$$

and

$$v = 0 \text{ at } y = h \quad (3.27)$$

We have

$$\Delta p_{f\_production} = \frac{\pi D_{tubing}L_{rod}\mu v_{rod}^2}{q_{production}\left(D_{tubing} - D_{rod}\right)} \quad (3.28)$$

where

$v_{\text{rod}}$ = sucker rod velocity.

The drag force between tubing wall and fluid can be calculated by

$$F_{\text{drag, tubing-fluid}} = \frac{\pi}{4}\left(D_{tubing}^2 - D_{rod}^2\right)\frac{\pi D_{tubing}L_{rod}\mu v_{rod}^2}{q_{production}\left(D_{tubing} - D_{rod}\right)} =$$

$$\frac{\pi^2\left(D_{tubing} + D_{rod}\right)D_{tubing}L_{rod}\mu v_{rod}^2}{4q_{production}} \quad (3.29)$$

### 3.3.2 Turbulent flow

If flow in the annulus is turbulent, the drag force on the flank of the piston can be analyzed by employing Reynolds number and friction factor.

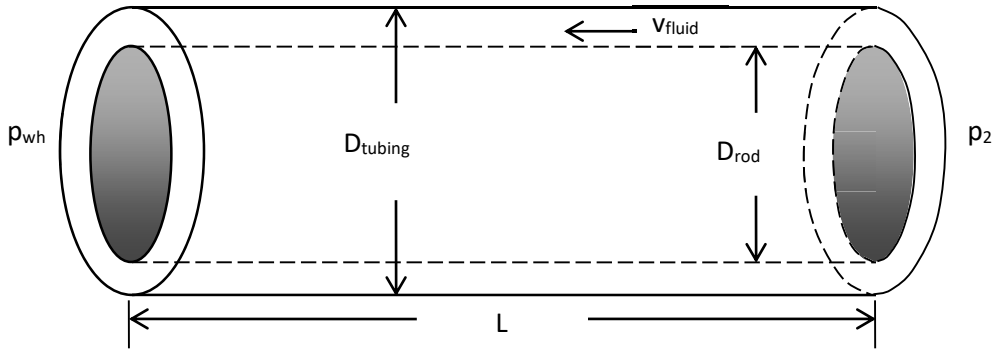


Figure 13 Schematic of fluid flow through an annulus between sucker rod and tubing

As discussed above, drag force between sucker rod and fluid is negligible. For **Fig. 12**, force balance requires that

$$\frac{\pi}{4}\left(D_{tubing}^2 - D_{rod}^2\right)\left(p_2 - \rho_f \frac{g}{g_c} L_{rod} - p_{wh}\right) = F_{\text{drag, tubing-fluid}} =$$

$$\tau_{tubing-fluid}\pi D_{tubing} L_{rod} \quad \text{..... (3.30)}$$

where

$\tau_{tubing-fluid}$= shear stress between tubing and fluid.

Introducing the definition of the Fanning friction factor, *f*, which is the ratio of the shear stress on the tubular wall applied by unit volume of fluid to its kinetic energy.

$$f = \frac{shear\ stress\ on\ the\ wall/volume\ of\ fluid}{kinetic\ energy/volume\ of\ fluid} \quad \text{..... (3.31)}$$

or

$$f = \frac{\tau_{tubing-fluid}}{\frac{1}{2}\rho_f \bar{v}_{fluid}^2} \quad (3.32)$$

where

$f$ = Fanning friction factor

$\bar{v}_{fluid}$ = average fluid velocity.

Rearranging **Eq. 3.32** yields

$$\tau_{tubing-fluid} = \frac{1}{2} f \rho_f \bar{v}_{fluid}^2 \quad (3.33)$$

The friction factor can be calculated by Chen's (1979) [27] equation:

$$f = \left\{ \frac{1}{4\log\left\{ \frac{\varepsilon}{3.7065} - \frac{5.0452}{N_{Re}} \log\left[ \frac{\varepsilon^{1.1098}}{2.8257} + \left( \frac{7.149}{N_{Re}} \right)^{0.8981} \right] \right\}} \right\}^2 \quad (3.34)$$

where $N_{\mathrm{Re}}$ is the Reynolds number, which is expressed as:

$$N_{Re} = \frac{D_e \rho_f \bar{v}_{fluid}}{\mu} \quad (3.35)$$

where

$D_e$ = equivalent hydraulic diameter

$\varepsilon$= relative roughness.

The equivalent hydraulic diameter $D_e$ is equal to four times the hydraulic radius, $r_H$.

$$D_e = 4r_H \quad \text{..... (3.36)}$$

and the hydraulic radius is defined as the ratio of the cross-sectional area to the wetted perimeter of the flow channel. In this case it is

$$r_H = \frac{\frac{\pi}{4}\left(D_{tubing}^2 - D_{rod}^2\right)}{\pi D_{tubing}} \quad \text{..... (3.37)}$$

where

$r_H$ = hydraulic radius.

Substituting **Eq. 3.36** into **3.35**, we have

$$N_{Re} = \frac{\pi\left(D_{tubing}^2 - D_{rod}^2\right)}{\pi D_{tubing}} \frac{\rho_f \bar{v}_{fluid}}{\mu} \quad \text{..... (3.38)}$$

Substituting **Eq. 3.38** into **3.34**, we have

$$f = \left\{ \frac{1}{4\log\left\{ \frac{\varepsilon}{3.7065} - \frac{5.0452}{\frac{\left(D_{tubing}^2 - D_{rod}^2\right)\rho_f \bar{v}_{fluid}}{D_{tubing}\ \mu}} \log\left[ \frac{\varepsilon^{1.1098}}{2.8257} + \left( \frac{7.149}{\frac{\left(D_{tubing}^2 - D_{rod}^2\right)\rho_f \bar{v}_{fluid}}{D_{tubing}\ \mu}} \right)^{0.8981} \right] \right\}} \right\}^2 \quad \text{..... (3.39)}$$

Substituting **Eq. 3.39** into **3.33**, we have

$$\tau_{tubing-fluid} =$$

$$\frac{1}{2}\left\{\frac{1}{4\log\left\{\frac{\varepsilon}{3.7065}-\frac{5.0452}{\frac{\left(D_{tubing}^2-D_{rod}^2\right)\rho_f\bar{v}_{fluid}}{D_{tubing}\quad\mu}}\log\left[\frac{\varepsilon^{1.1098}}{2.8257}+\left(\frac{7.149}{\frac{\left(D_{tubing}^2-D_{rod}^2\right)\rho_f\bar{v}_{fluid}}{D_{tubing}\quad\mu}}\right)^{0.8981}\right]\right\}}\right\}^2 \rho_f\bar{v}_{fluid}^2 \quad (3.40)$$

Thus, the drag force on the wall of the tubing is expressed as

$$F_{\text{drag, tubing-fluid}} =$$

$$\frac{\pi}{2}D_{tubing}L_{rod}\left\{\frac{1}{4\log\left\{\frac{\varepsilon}{3.7065}-\frac{5.0452}{\frac{\left(D_{tubing}^2-D_{rod}^2\right)\rho_f\bar{v}_{fluid}}{D_{tubing}\quad\mu}}\log\left[\frac{\varepsilon^{1.1098}}{2.8257}+\left(\frac{7.149}{\frac{\left(D_{tubing}^2-D_{rod}^2\right)\rho_f\bar{v}_{fluid}}{D_{tubing}\quad\mu}}\right)^{0.8981}\right]\right\}}\right\}^2 \rho_f\bar{v}_{fluid}^2$$

..... (3.41)

for turbulent flow in sucker rod-tubing annulus.

Average fluid velocity can be calculated from production rate.

**Drag forces between plunger/working barrel and fluid**

Drag forces applied on plunger/working barrel by fluid flow cause frictional pressure drop when fluid slips. The drag forces between plunger/working barrel and fluid can be calculated using equivalent slot concept as shown in **Fig. 13**. According to mass balance, the slippage rate and average slip velocity are.

$$q_{slip\_upstroke} = v_{plunger}A_{plunger} - q_{production}.. \quad (3.42)$$

$$\bar{v}_{slip\_upstroke} = \frac{v_{plunger}A_{plunger} - q_{production}}{\frac{\pi}{4}\left(D^2_{working\ barrel} - D^2_{plunger}\right)} \quad (3.43)$$

where

$D_{plunger}$= plunger diameter

$D_{working\ barrel}$= working barrel diameter

$v_{plunger}$= plunger velocity

$\bar{v}_{slip\_upstroke}$= average slip velocity in upstroke.

### 3.4.1 Laminar flow

For laminar flow, following the above steps we can obtain

$$A = Wh = \frac{\pi}{4}\left(D^2_{working\ barrel} - D^2_{plunger}\right) \quad (3.44)$$

where

$$W = \frac{\pi}{2}\left(D_{working\ barrel} + D_{plunger}\right) \quad (3.45)$$

and

$$h = \frac{1}{2}\left(D_{working\ barrel} - D_{plunger}\right) \quad (3.46)$$

As mentioned above, plunger velocity can be approximated by sucker rod velocity. The fluid velocity and shear stress distribution in the annulus can be depicted in **Fig. 13**. The forces applied on a controlled fluid volume are also illustrated in **Fig. 13**.

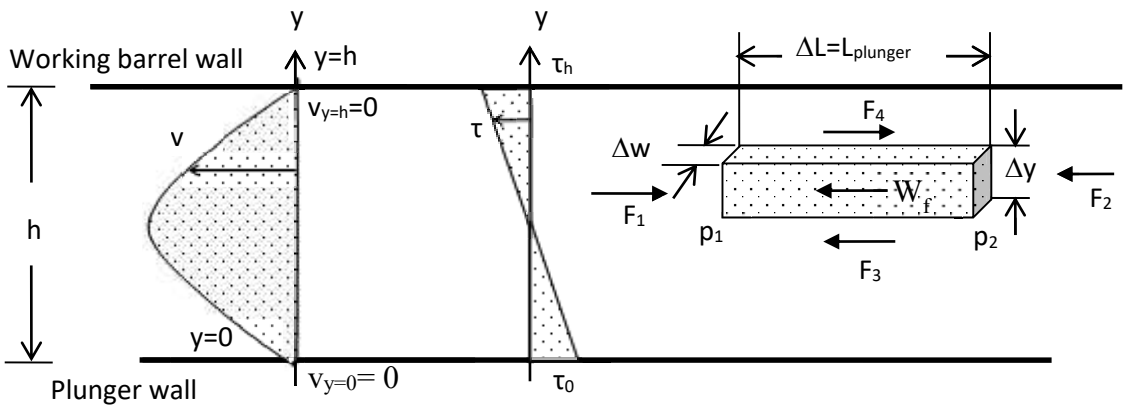


Figure 14 Free body diagram for a controlled fluid volume in a slot representing plunger-working barrel annulus

For a controlled fluid volume (**Fig. 13**) with width *Δw* and thickness *Δy*. Force equilibrium in vertical direction gives

$$F_1 + F_4 = F_2 + F_3 + W_f \ldots \quad (3.47)$$

where

$$F_1 = p_1 \Delta w \Delta y = p_2 \Delta w \Delta y - \frac{dp_f}{dL} \Delta L \Delta w \Delta y + \rho_f \frac{g}{g_c} \Delta L \Delta w \Delta y = \left(p_2 - \frac{dp_f}{dL} L_{plunger} + \rho_f \frac{g}{g_c} L_{plunger}\right) \Delta w \Delta y \ldots \quad (3.48)$$

$$F_2 = p_2 \Delta w \Delta y \ldots \quad (3.49)$$

$$F_3 = \tau_y \Delta w \Delta L = \tau_y \Delta w L_{plunger} \ldots \quad (3.50)$$

$$F_4 = \tau_{y+\Delta y} \Delta w \Delta L = \left(\tau_y + \frac{d\tau}{dy} \Delta y\right) \Delta w L_{plunger} \ldots \quad (3.51)$$

and

$$W_f = \rho_f \frac{g}{g_c} L_{plunger} \Delta w \Delta y \ldots \quad (3.52)$$

where

$\Delta L$= length of controlled fluid volume, in this case, length of fluid column is the plunger length, or $\Delta L = L_{plunger}$

$L_{plunger}$= plunger length

Substituting **Eqs. 48** through **52** into **Eq. 47** yields

$$\left(p_2 - \frac{dp_f}{dL} L_{plunger} + \rho_f \frac{g}{g_c} L_{plunger}\right) \Delta w \Delta y + \left(\tau_y + \frac{d\tau}{dy} \Delta y\right) \Delta w L_{plunger} = p_2 \Delta w \Delta y +$$

$$\tau_y \Delta w L_{plunger} + \rho_f \frac{g}{g_c} L_{plunger} \Delta w \Delta y. \quad (3.53)$$

Expanding and canceling out the same terms on both sides gives

$$\frac{dp_f}{dL} L_{plunger} \Delta w \Delta y = \frac{d\tau}{dy} \Delta y \Delta w L_{plunger}.. \quad (3.54)$$

Dividing **Eq. 54** by $L_{plunger} \Delta w \Delta y$, we have

$$\frac{dp_f}{dL} = \frac{d\tau}{dy}.. \quad (3.55)$$

Because d$p_f$/d$L$ is not a function of $y$, **Eq. 55** can be integrated with respect to $y$. Separating variables and integrating gives

$$\tau = y \frac{dp_f}{dL} + \tau_0. \quad (3.56)$$

where $\tau_0$ is the constant of integration that corresponds to the shear stress at $y$=0. From the definition of shear rate, $\dot{\gamma}$, we obtain

$$\dot{\gamma} = -\frac{dv}{dy}. \quad (3.57)$$

Combining **Eq. 56** with the definition of viscosity for Newtonian fluid gives

$$\tau = \mu\dot{\gamma} = -\mu\frac{dv}{dy} = y\frac{dp_f}{dL} + \tau_0 \quad (3.58)$$

Again, separating variable and integrating yields

$$v = -\frac{y^2}{2\mu}\frac{dp_f}{dL} - \frac{\tau_0 y}{\mu} + v_0 \quad (3.59)$$

where $v_0$ is the second constant of integration that corresponds to the fluid velocity at $y$=0. Applying the boundary condition

$$v = 0 \text{ at } y = 0 \quad (3.60)$$

we have

$$0 = -\frac{0^2}{2\mu}\frac{dp_f}{dL} - \frac{\tau_0(0)}{\mu} + v_0 \quad (3.61)$$

Similarly applying the boundary condition

$$v = 0 \text{ at } y = h \quad (3.62)$$

we have

$$0 = -\frac{h^2}{2\mu}\frac{dp_f}{dL} - \frac{\tau_0 h}{\mu} + v_0 \quad (3.63)$$

Therefore, the constants of integration $v_0$ and $\tau_0$ are

$$v_0 = 0 \quad (3.64)$$

and

$$\tau_0 = -\frac{h}{2}\frac{dp_f}{dL} \quad (3.65)$$

Substituting **Eqs.3.64** and **3.65** into **3.59** gives

$$v = \frac{1}{2\mu}\frac{dp_f}{dL}(hy - y^2) \ldots\ldots (3.66)$$

The flow rate $q$ is the product of velocity $v$ and area $A$. Integrating the control volume flow rate throughout the interval from 0 to $h$ we obtain total flow rate

$$q_{slip\_upstroke} = \int vdA = \int_0^h vWdy = \frac{W}{2\mu}\frac{dp_f}{dL}\int_0^h (hy - y^2)dy \ldots\ldots (3.67)$$

Integrating **Eq. 3.67** yields

$$q_{slip\_upstroke} = \frac{Wh^3}{12\mu}\frac{dp_f}{dL} \ldots\ldots (3.68)$$

Substituting **Eqs. 3.45** and **3.46** into **3.68**, we obtain

$$q_{slip\_upstroke} = \frac{\pi\left(D^2_{working\ barrel} - D^2_{plunger}\right)\left(D_{working\ barrel} - D_{plunger}\right)^2}{192\mu}\frac{dp_f}{dL} =$$

$$v_{plunger}A_{plunger} - q_{production} \ldots\ldots (3.69)$$

Expressing the slippage rate in terms of the mean flow velocity and solving for the frictional pressure gradient gives

$$\bar{v}_{slip\_upstroke} = \frac{q_{slip\_upstroke}}{\frac{\pi}{4}\left(D^2_{working\ barrel} - D^2_{plunger}\right)} = \frac{\left(D_{working\ barrel} - D_{plunger}\right)^2}{48\mu}\frac{dp_f}{dL} \ldots\ldots (3.70)$$

$$\frac{dp_f}{dL} = \frac{48\mu\bar{v}_{slip\_upstroke}}{\left(D_{working\ barrel} - D_{plunger}\right)^2} \ldots\ldots (3.71)$$

Integrating **Eq.3.71** we have friction pressure drop along the annulus

$$\Delta p_{f\_slip} = \int_0^{L_{plunger}} \frac{dp_f}{dL}dL = \frac{48\mu\bar{v}_{slip\_upstroke}L_{plunger}}{\left(D_{working\ barrel} - D_{plunger}\right)^2} \ldots\ldots (3.72)$$

The friction forces between plunger wall/working barrel and fluid can be calculated by

$$F_{\text{drag, plunger-fluid}} = \frac{\pi}{4}\left(D^2_{working\ barrel} - D^2_{plunger}\right)\Delta p_{f\_slip} =$$

$$\frac{12\pi\mu\left(D_{working\ barrel}+D_{plunger}\right)\bar{v}_{slip\_upstroke}L_{plunger}}{D_{working\ barrel}-D_{plunger}} \quad \text{(3.73)}$$

Average fluid slip velocity can be calculated from the difference between volume displaced by plunger and production rate as shown in **Eq. 3.43**.

### 3.4.2 Turbulent flow

Similar to the derivation of frictional force between tubing and fluid, the drag force between plunger/working barrel and fluid can be calculated by

$$F_{\text{drag, plunger-fluid}} = \frac{\pi}{2}\left(D_{working\ barrel} + D_{plunger}\right)L_{plunger}$$

$$\left\{\frac{1}{4\log\left\{\frac{\varepsilon}{3.7065} - \frac{5.0452}{\frac{\left(D^2_{working\ barrel}-D^2_{plunger}\right)\rho_f\bar{v}_{slip\_upstroke}}{\mu}}\log\left[\frac{\varepsilon^{1.1098}}{2.8257} + \left(\frac{7.149}{\frac{\left(D^2_{working\ barrel}-D^2_{plunger}\right)\rho_f\bar{v}_{slip\_upstroke}}{\mu}}\right)^{0.8981}\right]\right\}}\right\}^2$$

..... (3.74)

**Force on rod caused by acceleration**

In operation no force attributable to fluid acceleration is required. Force needed to accelerate the sucker rod and plunger in the upstroke can be calculated by

$$F_{\text{acceleration}} = \left(m_p + m_r\right)a \quad \text{..... (3.75)}$$

where

$a$ = acceleration factor

$m_p$ = mass of plunger

$m_r$ = mass of sucker rod

The acceleration factor can be calculated by (Svinos, 1983) [28]

$$a = A\ddot{\theta}_4 \quad (3.76)$$

where

$$\ddot{\theta}_4 = \dot{\theta}_4\left[\left(\dot{\theta}_2 - \dot{\theta}_3\right)\cot(\theta_2 - \theta_3) - \left(\dot{\theta}_3 - \dot{\theta}_4\right)\cot(\theta_3 - \theta_4)\right].. \quad (3.77)$$

for constant crank angular velocity, which is normal in operation.

$\theta_2, \theta_3$, and $\theta_4$ can be calculated by

$$\theta_2 = 2\pi - \theta + \alpha.. \quad (3.78)$$

$$\alpha = \sin^{-1}\left(\frac{I}{K}\right).. \quad (3.79)$$

$$\theta_3 = \cos^{-1}\left(\frac{P^2+L^2-C^2}{2PL}\right) - \beta.. \quad (3.80)$$

$$\theta_4 = \cos^{-1}\left(\frac{P^2-L^2-C^2}{2CL}\right) - \beta.. \quad (3.81)$$

$$L = \sqrt{K^2 + R^2 - 2KR\cos\theta_2}.. \quad (3.82)$$

$$\beta = \cos^{-1}\left(\frac{K^2+L^2-R^2}{2KL}\right) * j.. \quad (3.83)$$

where

$$j = \begin{cases} 1 \text{ for } 0 < \theta_2 < \pi \\ -1 \text{ for } \pi < \theta_2 < 2\pi \end{cases}.. \quad (3.84)$$

$\dot{\theta}_2, \dot{\theta}_3$ and $\dot{\theta}_4$ are the derivative of $\theta_2, \theta_3$, and $\theta_4$ with respect to time.

where

$\theta$ = crank shaft rotation angle.

Variables in **Eqs. 3.78** through **3.84** are defined by the layout and dimension of sucker rod pumping system (conventional unit) as shown in **Fig. 14**.

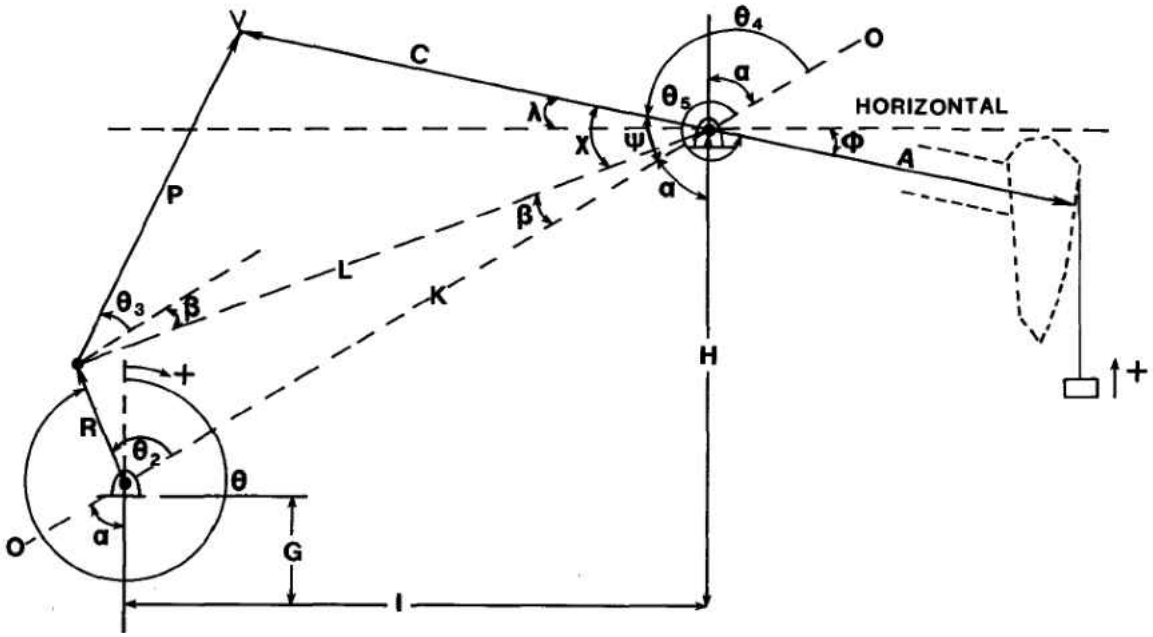


Figure 15 Geometric diagram of conventional units **[29]**

**Pressure below plunger (upward force acting on rod by fluid)**

When plunger moves up, traveling valve closes and standing valve opens. The void below plunger caused by the upward movement of plunger leads to the expansion of fluid and flow of reservoir fluid into working barrel. The pressure below plunger, $p_1$, depends on the plunger velocity and reservoir capacity to refill the working barrel. The flow rate of reservoir fluid from bottomhole into working barrel can be calculated by choke performance, where port of working barrel can be treated as a choke

$$q = CA_{standing\ valve}\sqrt{\frac{2g_c(p_{wf}-p_1)}{\rho_f}} \quad (3.85)$$

where

$C$ = choke discharge coefficient

$A_{\text{standing valve}}$ = cross-sectional area of choke (or standing valve)

$g_c$ = unit conversion costant

$p_{wf}$ = flowing bottomhole pressure

$q$ = flow rate from bottomhole into working barrel.

Reservoir fluid flow rate can also be calculated by reservoir inflow performance, which is

$$q = J(p_e - p_{wf}) \quad (3.86)$$

where

$J$ = productivity index

$p_e$ = reservoir pressure.

The definition of fluid compressibility gives

$$c_f = -\frac{1}{V}\frac{dV}{dp} \quad (3.87)$$

where

$p$ = pressure

$V$ = fluid volume

$c_f$ = fluid compressibility.

The pressure below plunger is related to the change of volume below plunger (or plunger velocity) and the expansion of fluid below plunger. Fluid volume in **Eq. 3.87** is the fluid

volume flow from bottomhole into working barrel during time interval $\Delta t$. **Eq. 3.87** can be rewritten into

$$A_{plunger} v_{plunger} = -c_f \left(q + q_{slip\_upstroke}\right) \Delta t \frac{dp}{dt} \quad \text{(3.88)}$$

At the beginning of upstroke, $p_1$ is equilibrium with flowing bottomhole pressure, or $p_1 = p_{wf}$, then **Eq. 3.88** can be expressed as

$$A_{plunger} v_{plunger} = c_f \left(q + q_{slip\_upstroke}\right) \left(p_{wf} - p_1\right) \quad \text{(3.89)}$$

Solving **Eqs. 3.85, 3.86**, and **3.89** simultaneously one can obtain $q$, $p_{wf}$, and $p_1$.

At this stage, all variables in **Eq. 3.1** have been calculated. The polished rod load can be estimated for the upstroke.

Companies may use tapered string to reduce polished rod load and energy consumption to operate pumping system. Through the proposed models, engineers can predict the possible failure point for rod string by analyzing load along the whole string. The proposed models are significant to the cyclic fatigue and failure analysis of rod in sucker rod pumping system. They are useful tool to design the tapered rod string to minimize the maximum rod load while achieving optimum rod string life.

# CHAPTER 4

# IV. EXPERIMENT

## Experiment Design

The two-phase flow experiment could be used to theoretically predict the flow parameters such as: flow rate, static pressure, and temperature. It is useful in predicting the shut-in pressure and in seeing the flow regime change after we shut the well. As well, the system could predict how the flow regime and pressure change when we reopen the valve. In this section, we designed an experiment of two-phase flow to study this topic.

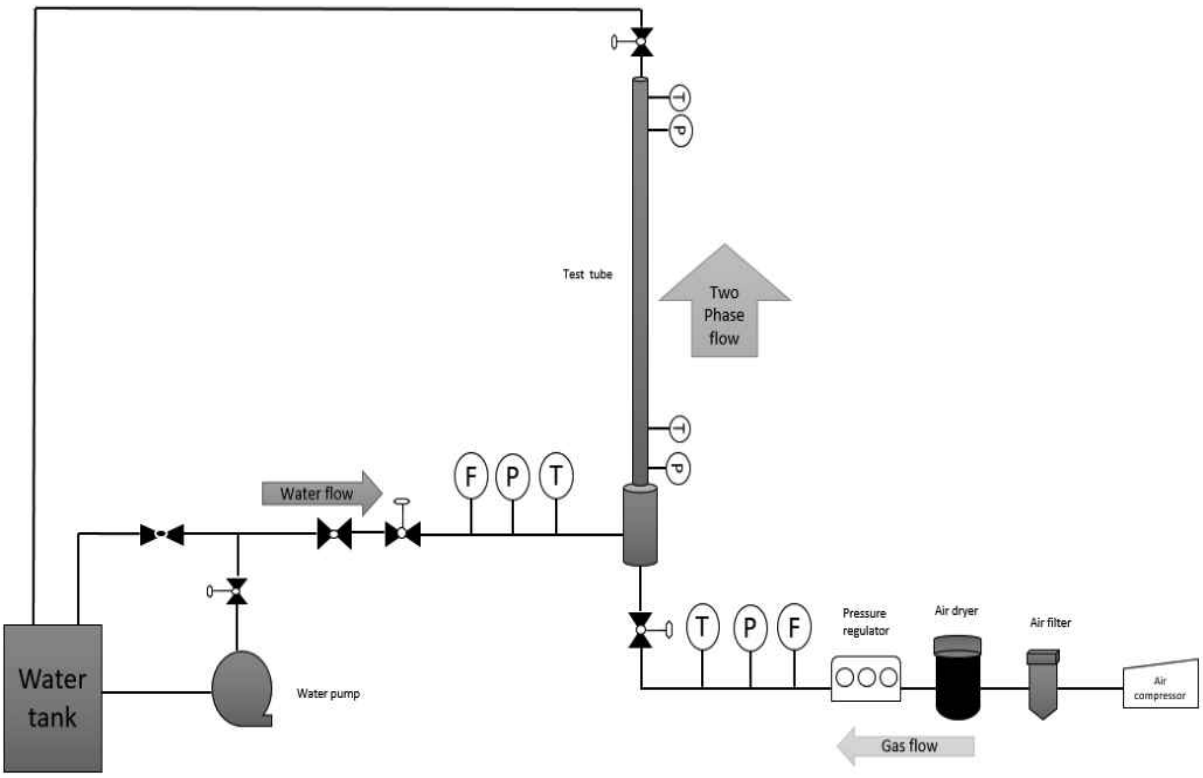


Figure 16 Experimental apparatus

Figure 17 Experimental apparatus in the lab

## Description of experiment equipment

This experimental design consists several major components:

- Water supply system
- Gas supply system
- A flow loop and test tube
- General instrumentation

### Water supply system

The tap water in the laboratory is filtered and then inject into the water tank which is about $1m^3$. The filtered water was recirculated in the system. Water pump motor I used can be

wired for either 230v or 460v at 60Hz power. The flow rate of this water pump is 9480 GPH which could make the liquid flow to the maximum of 5 m/s.

We use the stop valve and ball valve work together to control the inlet velocity of the water. After I shut down the water pump in the loop, the water can go back to the water tank without going through the pump. The water goes through another pipe that is designed to bypass the water pump.

During the experiment, water would be heated up because of the working pump. To fix this problem, we continuously add cold water to the top of the water tank and extract heated water from the bottom of the tank.

The flow rate, inlet pressure and temperature could be monitored by the gauge installed on the water supply pump.

**Gas supply system**

Air was provided by a 15 HP 120Gallon two stage air compressor manufactured by Ingersoll Rand. The maximum flow rate is 50 CFM which makes the maximum air flow rate about 10m/s in the test tube. By integrating different water flow rates, we could get all the types of flow patterns.

The tank to contain the air holds 120 Gallons, and is 83 inches in length and 36 inches in width which helps us to smooth out the flow oscillation. When the air exits the tank it goes through a ¾ inch pipe and a unit combines air dryer, filter and a pressure regulator. With the help of the dryer and filter, the contaminants from the atmosphere get eliminated,

and the clean and dry air could help us get a more accurate result from in the flow meter insertion probe of the downstream. The data will be collected by the computer over a long period of time.

**Test section**

The length of the test section is an important parameter for the two-phase flow experiment. The longer test tube means the fluid flow will become fully developed just like the vertical well thousands of meters away from the surface. All of the flow pattern we introduced before could occur in the wellbore.

In our experiment, we use different diameters of clear PVC pipes to make the flow pattern visible and a 6ft length to make the fluid flow develop the fluid flow. The details of the tube can be found in this Table 1.

Table 1 Test tube

| Pipe size(inch) | OD(inch) | Design pressure(psi) |
|---|---|---|
| 1" | 1.3" | 220 |
| 2" | 2.4" | 140 |
| 3" | 3.5" | 130 |

There have been a lot of scholars who have performed the two-phase flow experiment to test the pressure drop both in horizontal and vertical pipes.

Table 2 Previous experimental database for two phase flow analysis

| Author | Flow direction | Pipe Diameter(mm) | Gas rate(m/s) | Liquid rate(m/s) |
|---|---|---|---|---|
| Huang(1993) [30] | Horizontal | 50.3 | 3.74-6.59 | 3.74-6.598 |
| Mohamed Limayem Lamari(2001) [31] | Horizontal | 25.4 | 0.02-3.4 | 0.005-4.9 |
| Bowden and Yang(2016) [32] | Horizontal | 50.8 | 3.50-5.42 | 3.5-5.42 |
| Shiba and Yamazaki (1967) [33] | Vertical | 25 | 0.06-119 | 0.18-3.66 |
| Oshhinowo and Charles(1974) [34] | Vertical | 25.2 | 0-28.8 | 0.01-1.98 |
| Jing Zhou (2013) [35] | Vertical | 50.8 | 0.3-10.3 | 0.15-0.91 |

In our study, we designed our study to use four different kinds of test tube to compare the flow regime and pressure drop differences between them. Also we measured the gas superficial velocity ranging from 0.1-9.6 m/s, and water superficial velocity ranging from 0.1-8.2 m/s. Due to the limitation of the previous database, we have a larger range of gas and liquid superficial velocities and various and larger test tubes with diameters of 25.4mm, 50.8mm, 76.2mm.

**Experiment procedure**

1. Make sure all the equipment and valves in the loop are in good condition.
2. Run water pump to have single phase flow in the loop.
3. Turn on air compressor and keep valves fully closed in air supply system until the air pressure is high enough.
4. Open the valves and combine two phases in the mixer.

5. Read pressure and flow rate until the number remain steady.
6. Close the valves in air supply system
7. Shut down air compressor
8. Shut down the water pump

When we run this two-phase flow experiment, there are several points to pay more attention.

[1] Close the valves on the air pipe until the air inlet pressure is higher than the water inlet pressure. This is to prevent the water coming into air supply system and causing serious problems to the air flow meter.

[2] Use glove valve to control the flow rate and make ball valve fully opened or closed.

[3] Open the air dryer right before we run air compressor

[4] Shut down air compressor first, to prevent the water in the system from coming out from the vent on top of the loop.

## Measurements of Flow Parameters

### Air Mass Flow Rates

The air flow meter we bought could monitor and record flow, pressure, temperature, and total air consumption, simultaneously. All the parameters will transfer to computer directly. The pressure sensor range is from 0 to 250 psi. And temperature resolution is less than 0.1˚C.

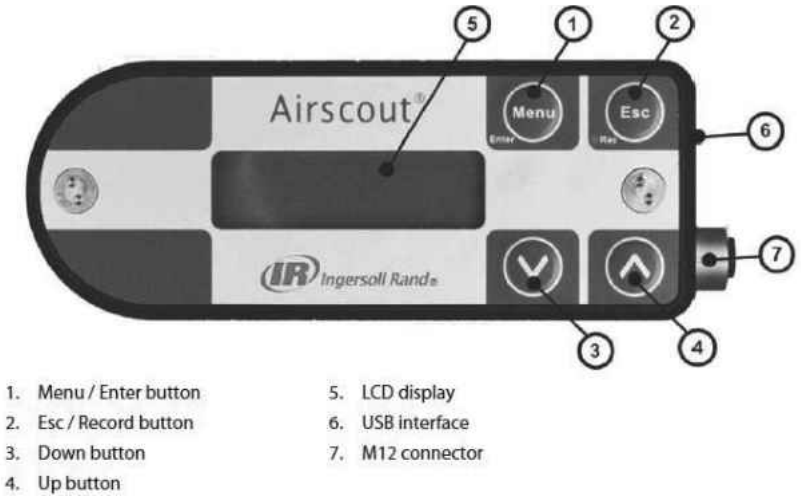


Figure 18 Air flow meter [36]

**Water flow rates**

The water flow meter we used tests the flow rate from 20-200 GPM. To get rid of turbulent flow influence, we connect a 20 inch straight PVC pipe in the upstream of the turbine and a 10 inch straight PVC pipe in the downstream of the turbine.


Figure 19 Water flow meter [37]

**Static pressure**


Figure 20 Pressure gauge [38]

The range of this gauge is from 0 to 200 psi. We use this gauge to test the water inlet pressure and test tube pressure drop. The display units of this gauge could be psi, bar, in.Hg, kpa, kg/cm2. And the resolution would be ¼% first half of range and ½% second half of range. The operating temperature is from -15 to 150 degrees Fahrenheit.

# CHAPTER 5

## V. SIMULATION RESULT AND ANALYSIS

In this section, we introduce the results from Ansys-Fluent. When combining with different air and water superficial velocities, all kinds of flow regimes would take place such as bubble flow, slug flow, churn flow, and annular flow. Also, we compare each simulation result with the vertical upwards flow pattern map as mentioned before.

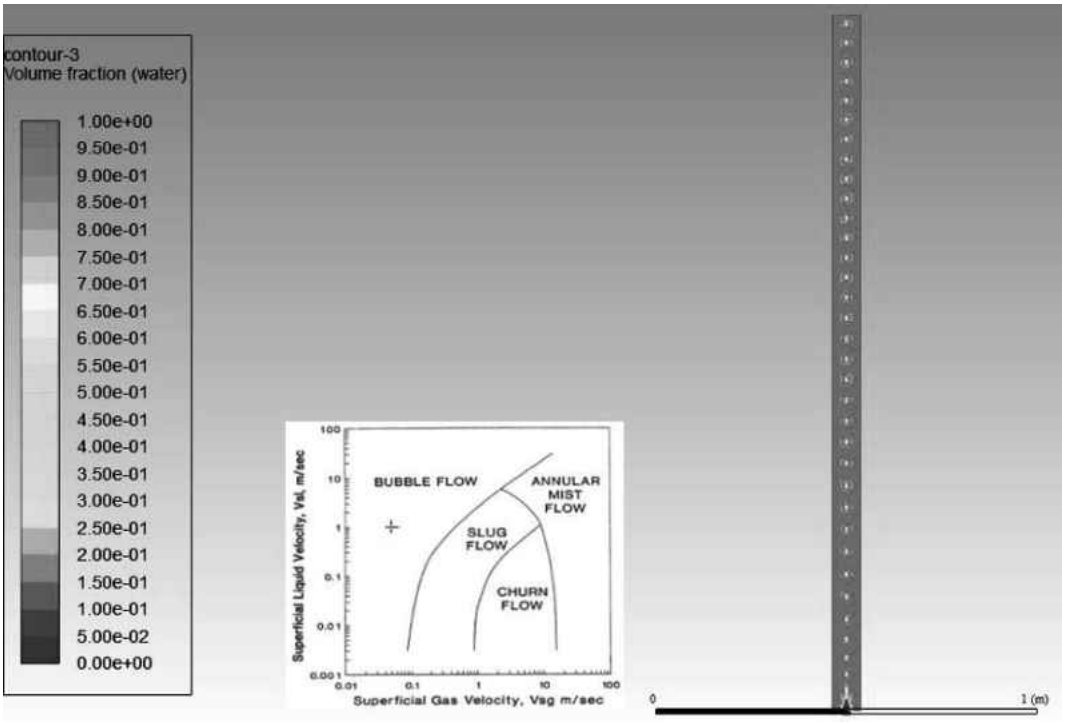


Figure 21 Gas superficial velocity 0.05 m/s, Water superficial velocity 1 m/s

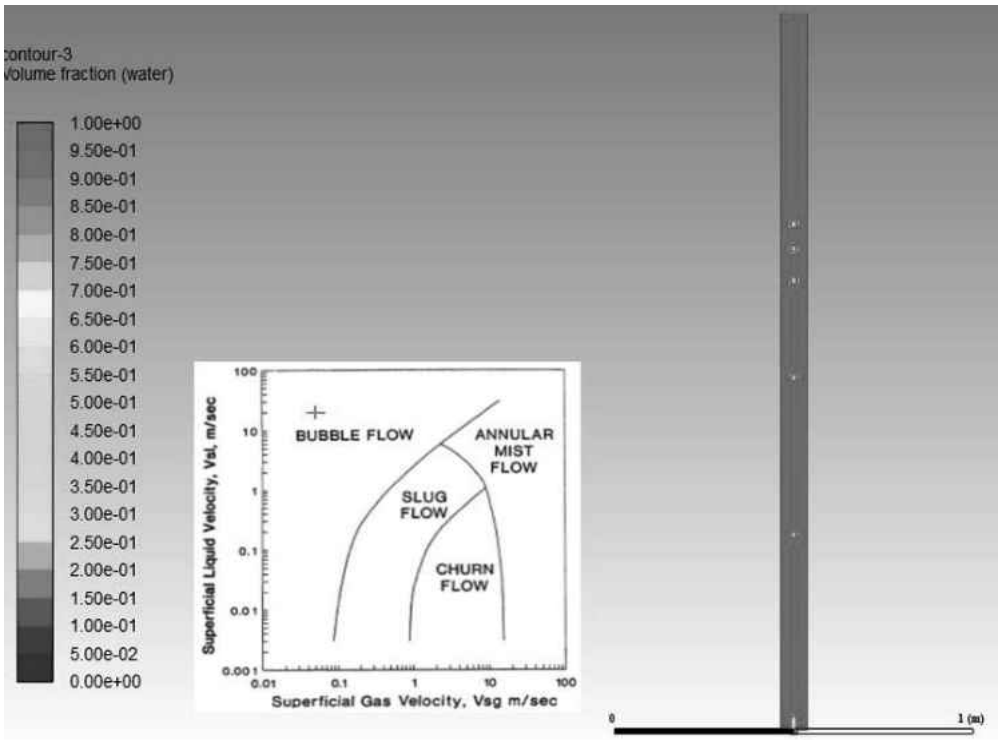


Figure 22 Gas superficial velocity 0.05 m/s, Water superficial velocity 20 m/s

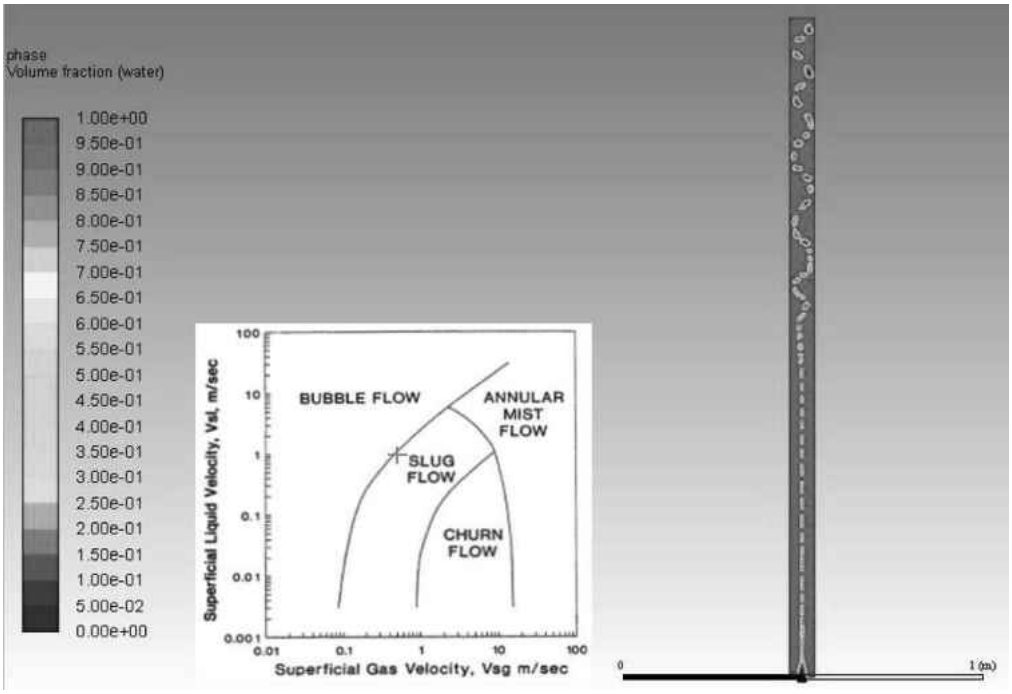


Figure 23 Gas superficial velocity 0.5 m/s, Water superficial velocity 1m/s

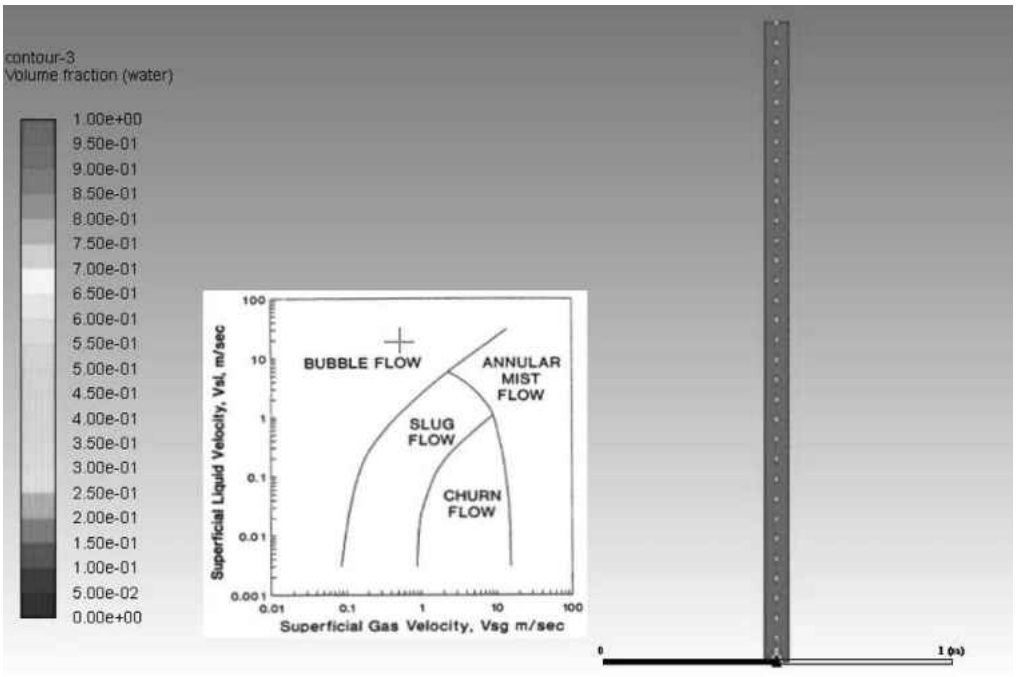


Figure 24 Gas superficial velocity 0.5m/s, Water superficial velocity 20m/s

Figure 25 Bubble flow

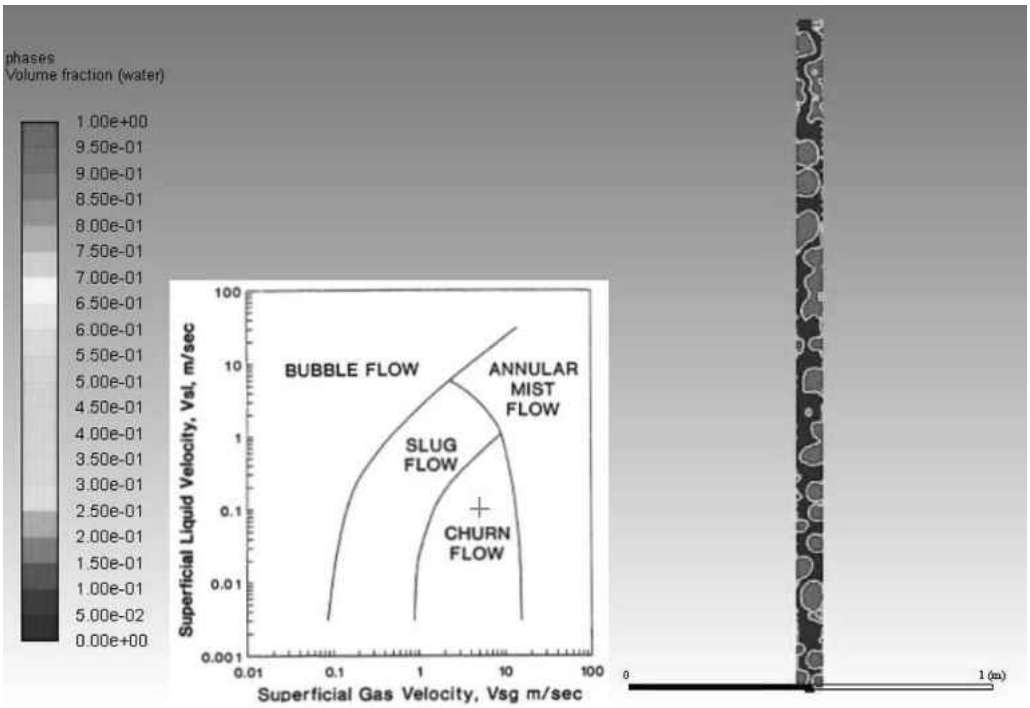


Figure 26 Gas superficial velocity 5m/s, Water superficial velocity 0.1m/s

Figure 27 Churn flow

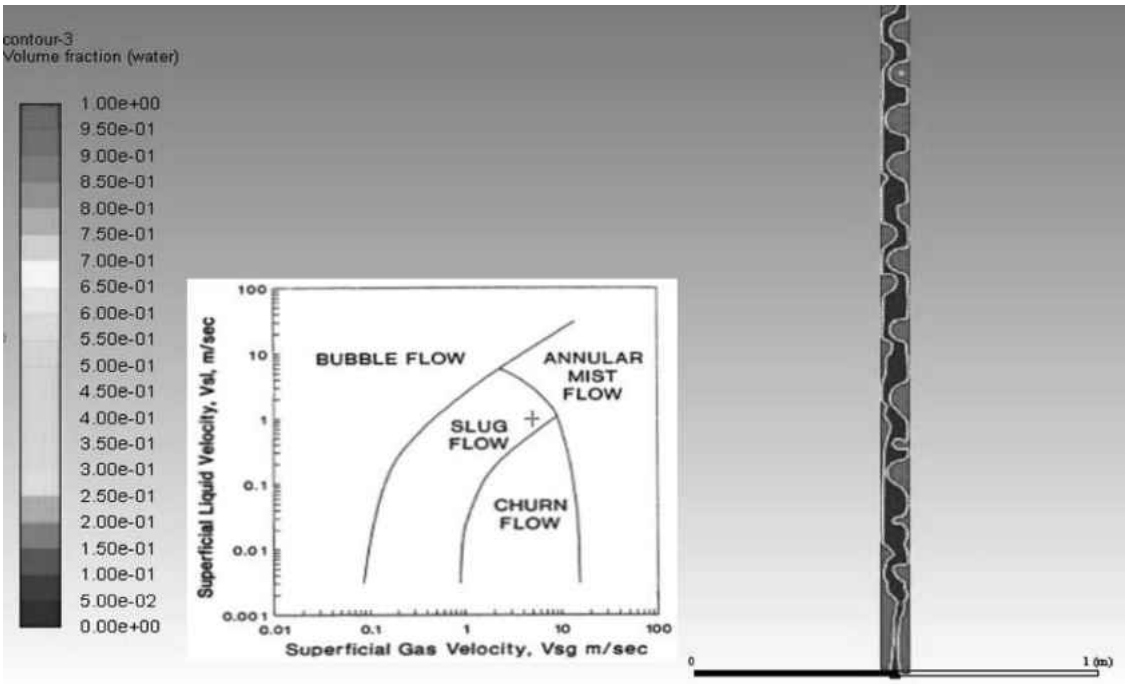


Figure 28 Gas superficial velocity 5m/s, Water superficial velocity 1m/s

Figure 29 Taylor bubble

Figure 30 Slug flow

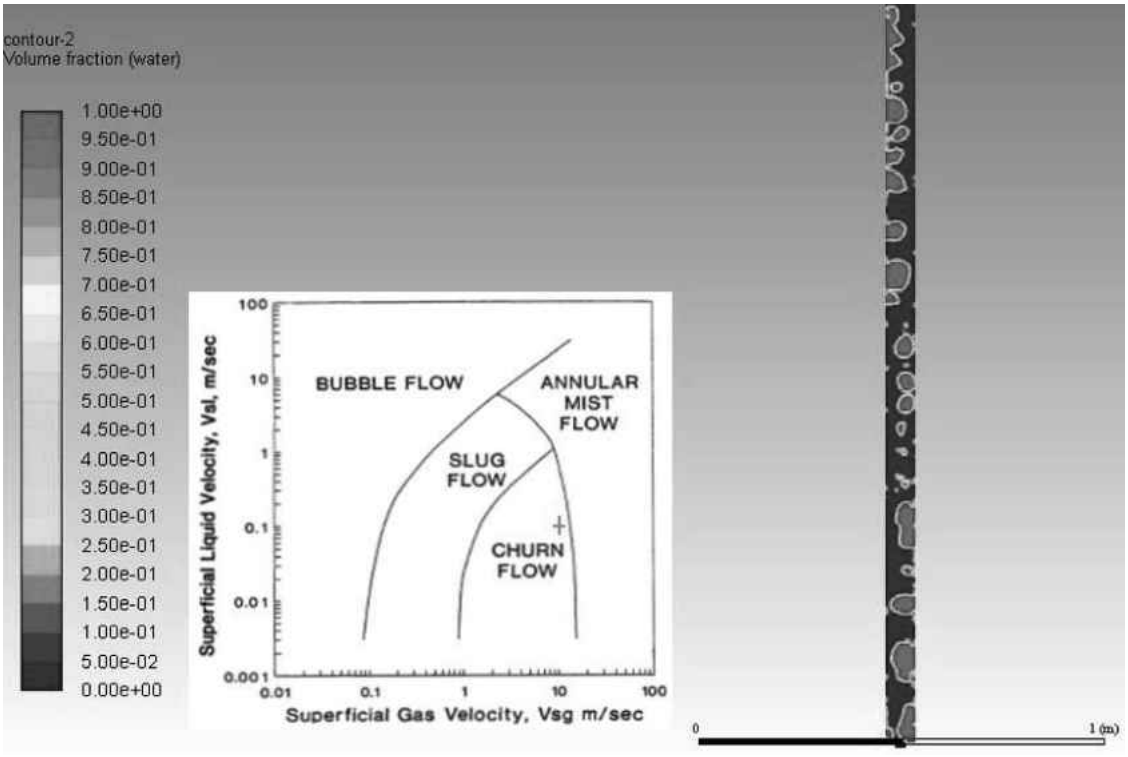


Figure 31 Gas superficial velocity 10m/s, Water superficial velocity 0.1m/s

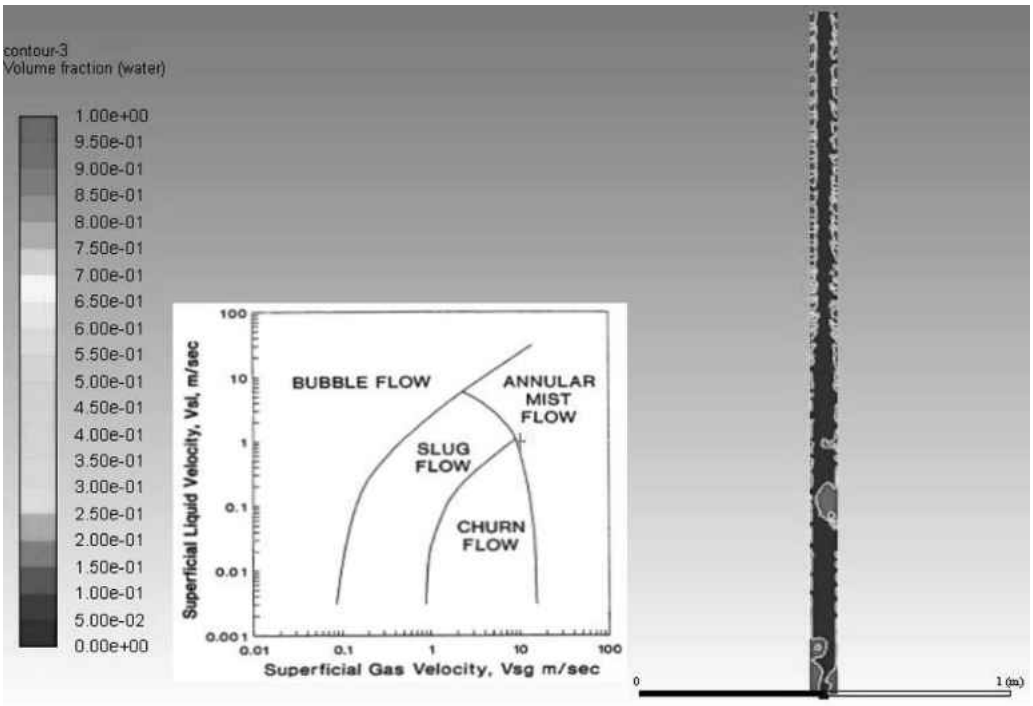


Figure 32 Gas superficial velocity 10m/s, Water superficial velocity 0.1m/s

Figure 33 Annular flow

From Figure 21 to 33, we could see the phase change happening and different kinds of flow regime. As we know, there are three critical elements that influence flow pattern: channel size, orientation, and phase changing process. After testing different flow regimes by this two-phase model in Ansys, we found the flow pattern shown in the software is similar with the existing flow.

When the gas superficial velocity is 0.5m/s, and the liquid phase superficial velocity is changed from 0.01 to 20 m/s, flow pattern would be bubble flow and change to dispersed bubbly flow with higher liquid flow velocity. Because of increasing continuous liquid phase superficial velocity, the bubbles could be smaller and separated with each other.

When the gas flow rate is 10 m/s, the liquid phase flow rate changing from 0.1 to 20 m/s, the flow pattern is changed from churn to annular flow after 30 seconds flow upwards in the simulation.

When the gas flow rate is 5 m/s, and liquid phase flow rate is 0.01~20 m/s, the slug flow and churn flow will take place. In this flow pattern large bubbles are separated by the liquid phase and the pressure oscillations within pipes happened because of slug flow. For example in Figures 34, 35. The pressure drop in bubble flow (gas superficial velocity of 0.05m/s, water superficial velocity of 10 m/s) and slug flow (gas superficial velocity of 2m/s, water superficial velocity of 1 m/s) both of these two results are tested in a 3 inch pipe.

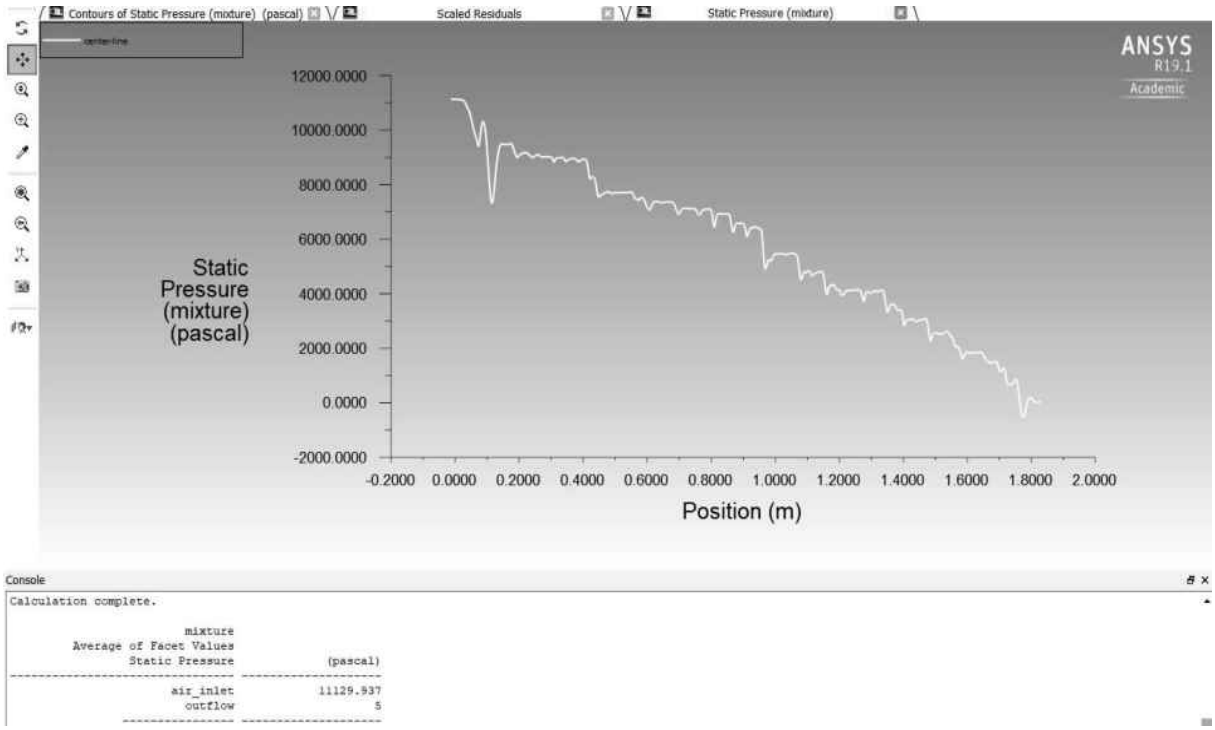


Figure 34 Slug flow pressure drop in the center line of the pipe

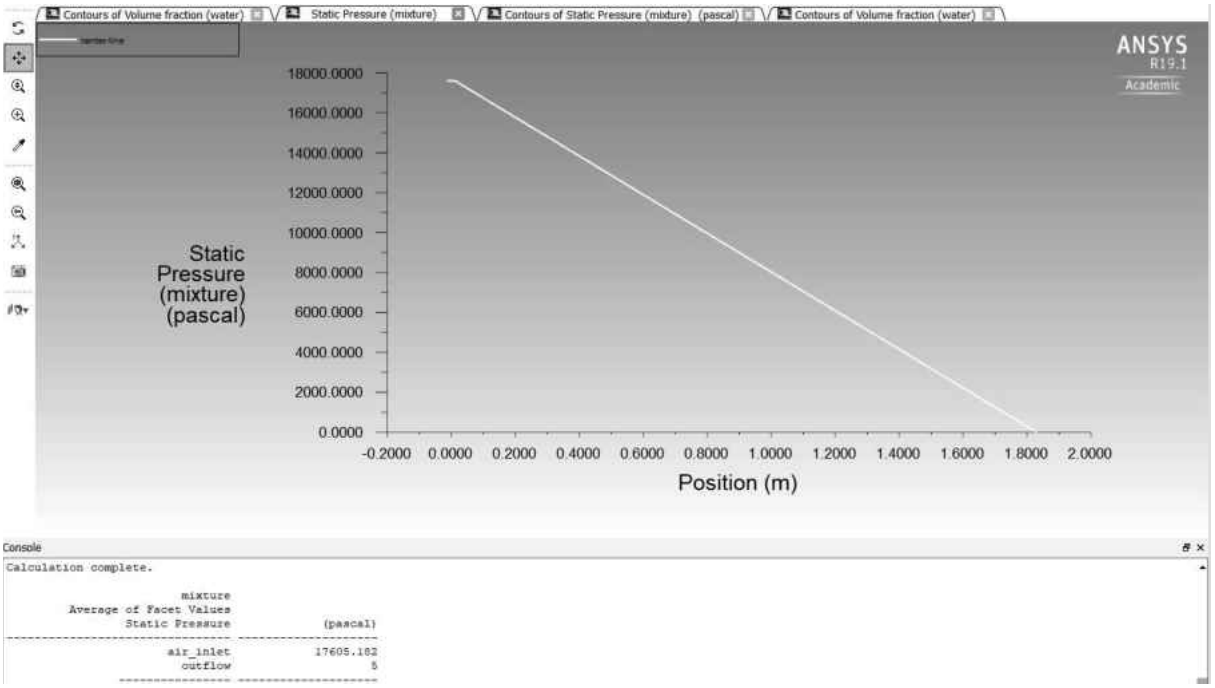


Figure 35 Bubble flow pressure drop in the center line of the pipe

Also, we would use these models to do further research and test effect factors of pressure drop in the test tube such as pipe size, water superficial velocity, gas superficial velocity, flow regime.

In Ansys-fluent, we integrate water-air surface tension and use time step to simulate flow regime change in a period of time.

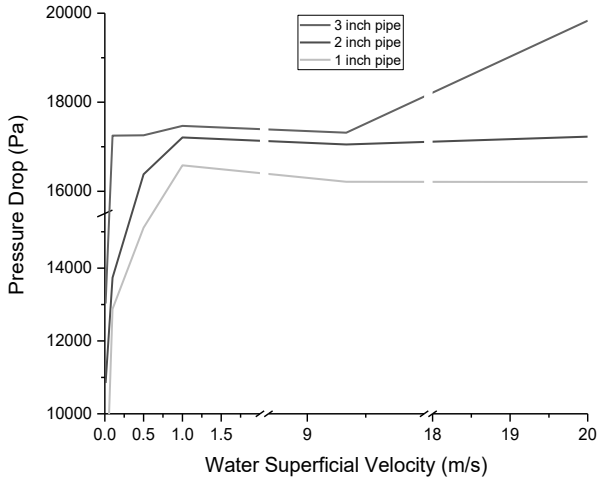


Figure 36 Gas superficial velocity is 0.05 m/s

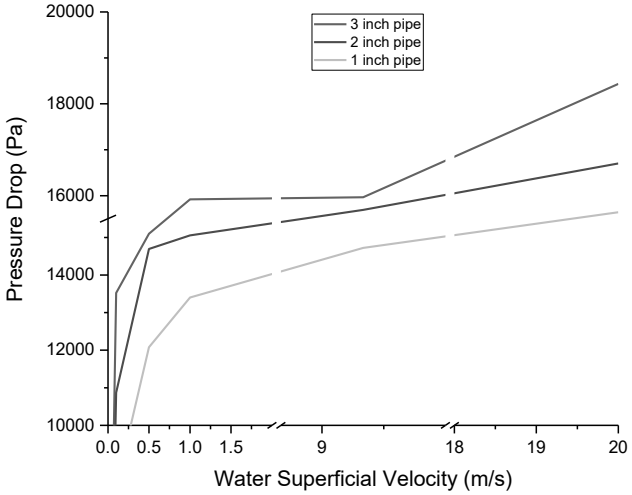


Figure 37 Gas superficial velocity is 0.5 m/s

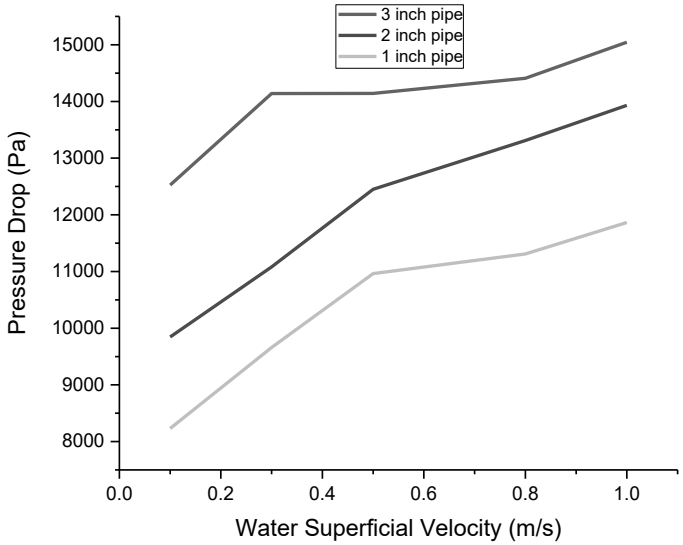


Figure 38 Gas superficial velocity is 1 m/s

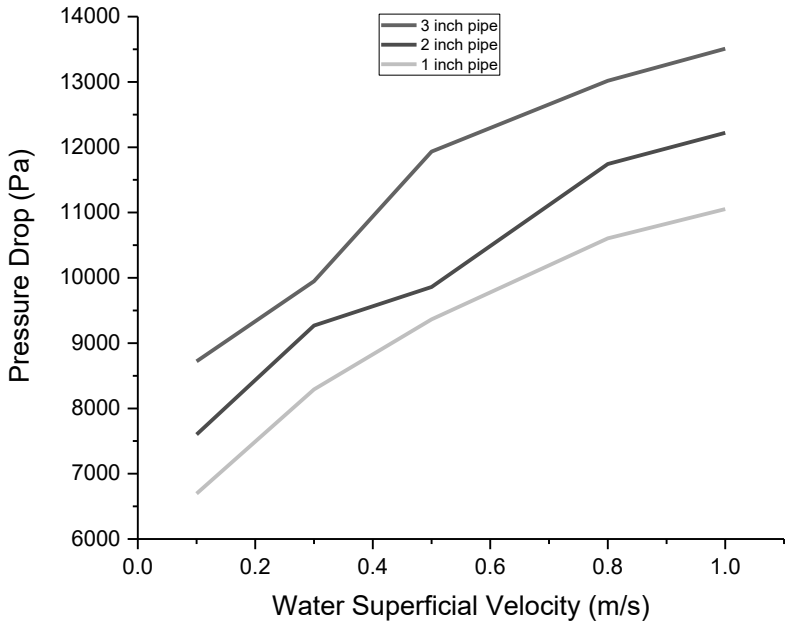


Figure 39 Gas superficial velocity is 2 m/s

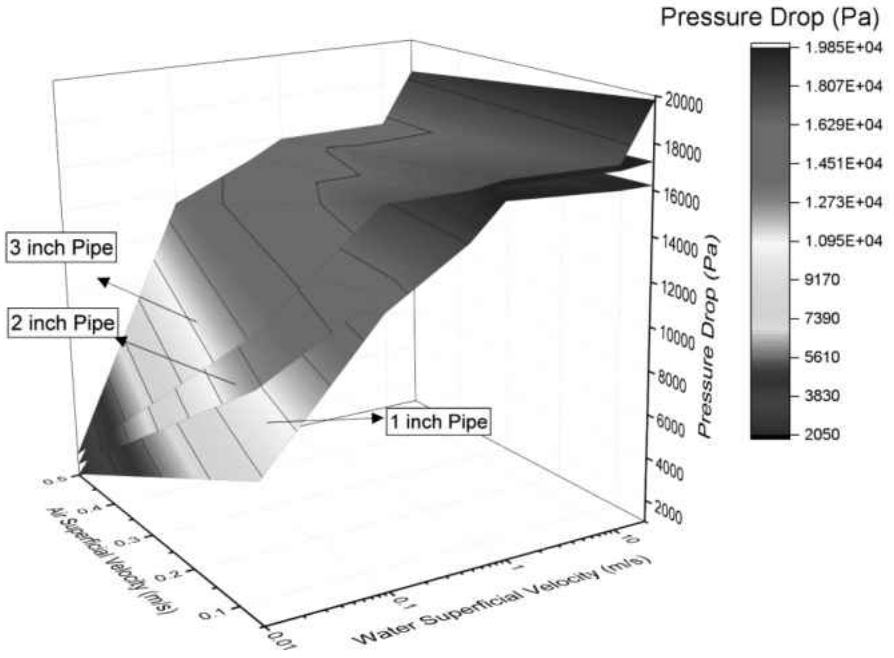


Figure 40 Bubble flow pressure drop simulation

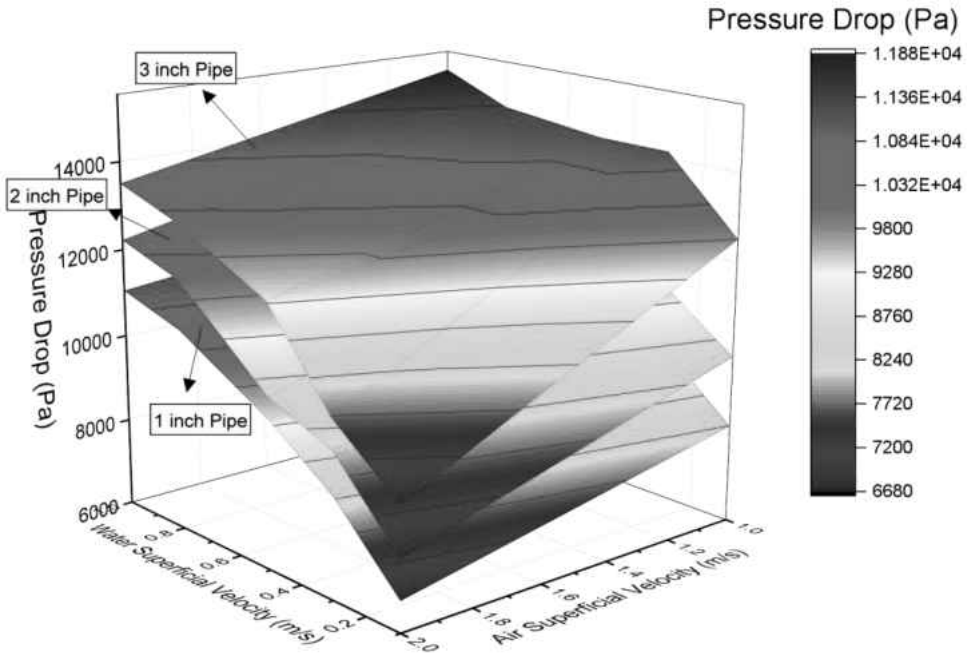


Figure 41 Slug flow pressure drop simulation

In this section, I use a 6 feet test tube and the diameters are varied: 1 inch, 2 inches, and 3 inches. Water superficial velocity ranges from 0.01 to 20 m/s and the gas superficial velocity is changing from 0.05 to 10 m/s. Both bubble flow and slug flow take place in the test tube. From the 2D graph, we known that in a certain gas superficial velocity, the higher water superficial velocity will cause a greater pressure-drop in the test tube. And when the water superficial velocity increases to 1 m/s, they are not smoothly changed because the fluid flow touches the boundary of bubble-slug flow and become unstable.

It is more clearly seen in the 3D graph that the larger diameter of the tube and the higher water superficial velocity result in a higher pressure-drop in the tube.

To compare the results we get from simulation with the experiment, we keep the water flow rate at 12.66 GPM while changing air flow rate from 2.0 to 3.8 SCFM, finding that the pressure-drop declined from 4.5 psi to 3 psi. Also, when we keep the air flow rate at 0.2 SCFM and change the water flow rate from, 8.4 to 0.7 GPM, the pressure-drop changes from 3.6 psi to 2.1 psi. The experiment results coincide with the simulation result.

# CHAPTER 6

# VI. CONCLUSION AND RECOMMENDATIONS

## Conclusion

In this study, I introduce the development of flow pattern maps and different approaches to calculate pressure-drop in the pipe. Also, I propose a more general model for sucker rod pumping system. Including friction force due to the movement of the plunger, the rod, buoyant force, and gravity force, viscous fluid in the model.

With literature reviews and contact with engineers from several companies, I already set up the construction of multi-phase flow loop experiment in the laboratory, which could generate all kinds of flow regime in the pipe.

After designing the two-phase flow loop, we compared each result with the vertical upwards flow pattern map (Dukler and Taitel [6]) to test the modeling in the software. The pressure drop analyzed different flow patterns and found the pressure oscillations take place in slug flow and pressure-drop is stable in bubble flow. The pressure-drop increased with a larger diameter of the tube, higher water superficial velocity, and lower air superficial velocity. Compared with air superficial velocity, the water superficial velocity has a dramatic influence on pressure-drop because of the gravity.

## Recommendations for Future Work

1. For further development, it is better to add a pressure transmitter to test the pressure-drop with time.
2. To get more accurate results, flow meter transmitters are also needed in the system, so data could be collected by a computer automatically.
3. Investigate the proper equipment and new methods to test more fluid properties.
4. Modify of the Fluent Model to predict the phase change and pressure gradient in the test tube.
5. Heating up the tube to measure temperature influence of the fluid flow.

## References


[1] Baker, "Simultaneous Flow of Oil and Gas," *Oil and Gas Journal,* vol. 53, pp. 185-195, 1954.

[2] A. S. L.P. Golan, "Two-Phase Vertical Flow Maps," in *Proceedings of the institution of Mechanical Engineers*, 1969.

[3] S. Company, "GAS/LIQUID SEPARATORS - TYPE SELECTION AND DESIGN RULES," *Design and Engineering Practice,* pp. 2-100, 12 2007.

[4] T. C. Oshinowo, "Vertical two-phase flow, flow pattern correlations," *Journal of Chemical Engineering,* vol. 52, pp. 25-35, 1974.

[5] G. R. D. Hewitt, "Studies of two-phase flow patterns by simultaneous x-ray and flast photography," United Kingdom, 1969.

[6] Y. A.E. Duler, "Flow regime transitions for vertical upward gas liquid flow: a preliminary approach through physical modeling," Progress Report No.2, NUREG-0163, 1977.

[7] Weisman.J, "Chapter 15 Two-phse flow patterns," in *Handbook of Fluids in Motion*, Ann Arbor, Mich. Ann Arbor Science, 1983.

[8] C. P. Milad Darzi, "Experimental Visualization and Numerical Simulation of Liquid-Gas Two-Phase Flows in a Horizontal Pipe," in *ASME 2017 International Mechanical Engineering Congress and Exposition*, Tampa, Florida, 2017.

[9] N. H. T. G.E. Hewitt, Annular Two-Phase Flow, Oxford: Elsevier Science, 1970.

[10] R. F. L. A. E. Bergles, "Critical-Heat-Flux and Flow-Pattern Observations for Low-Pressure Water Flowing in Tubes," *Journal of Heat transfer,* vol. 89, pp. 69-74, 1967.

[11] A. Bergles, "Two phase flow structure observations for high pressure water in a rod bundle," in *Winter annual meetings*, 1969.

[12] D. G. J.M, Measuring Techniques in Gas-Liquid Two-Phase Flows, Nancy, 1983.

[13] T. C. B. K.H.Chien, "Void fraction measurement by using the side-tube method," *Flow Measurement and Instrumentation,* vol. 8, no. 2, pp. 103-112, 1997.

[14] A. R. Ugandhar Puli, "An image analysis technique for determination of void fraction in subcooled flow boiling of water in horizontal annulus at high pressures," *International Journal of Heat and Fluid Flow,* vol. 38, pp. 180-189, 2012.

[15] H. K. T. I. Tomio Okawaw, "Simultaneous measurement of void fraction and fundamental bubble parameters in subcooled flow boiling," *Nuclear Engineering and Design,* vol. 237, pp. 1016-1024, 2006.

[16] J. B. L.-w. H. T. M. Craig Gerardi, "Measurement of nucleation site density, bubble departure diameter and frequency in pool boiling of water using high-speed infrared and optical cameras," in *ECI international Conference on Boiling Heat Transfer*, Brazil, 2009.

[17] X. X. M. I. S.Kim, "Development of the miniaturized four-sensor conductivity probe and the signal processing scheme," *International journal of heat and mass transfer,* vol. 43, pp. 4101-4118, 2000.

[18] H. d. Burak dibek, "determination of void fraction by image processing," *Journal of the Faculty of Engineering,* vol. 22, no. 3, 2017.

[19] R. a. M. R. Lockhart, "Proposed Correlation of Data for Isothermal Two Phase Flow, Two Component Flow in Pipes," *Chemical Engineering Progress,* pp. 39-48, 1949.

[20] K. H. HMüller-Steinhagen, "A simple friction pressure drop correlation for two-phase flow in pipes," *Chemical Engineering Progress,* vol. 20, no. 6, pp. 297-308, 1986.

[21] K. A. G. W. Govier, The flow of complex mixtures in pipes, Van Nostrand Reinhold Company (1972), 1972.

[22] G. ,. R. D. Hewitt, "Studies of two-phase flow patterns by simultaneous X-ray and flash photography," *Atomic Energy Research Establishment,* pp. ÄERE - M 2159, 1969.

[23] P. J.M.Delhaye, "Interfacial area in bubbly flow: experimental data and correlations," *Nuclear Engineering and Design,* vol. 151, no. 1, pp. 65-77, 1994.

[24] W. W. W. &. H. McAdams, "Vaporization inside horizontal tubes II-benzeneoil mixture," *Trans. ASME,* vol. 39, pp. 39-48, 1949.

[25] A. E. D. M. W. I. R. G. Cleveland, "Frictional pressure drop in two-phase flow: B. An approach through similarity analysis," *AIChE J,* vol. 10, pp. 38-51, 1964.

[26] D. &. W. P. Beattie, "Simple two-phase frictional pressure drop calculation method," *Int. J. Multiphase Flow,* vol. 8, no. 1, pp. 83-87, 1982.

[27] N. H. Chen, "An Explicit Equation for Friction Factor in Pipe," *industrial & Engineering Chemistry Fundamentals,* vol. 18, no. 3, pp. 296-297, 1979.

[28] J.G.Svinos, "Exact Kinematic Analysis of Pumping Units," in *Society of Petroleum Engineers*, Francisco, California, 1983.

[29] J. Svinos, "Exact Kinematic Analysis of Pumping Units," in *Society of Petroleum Engineers*, 1983.

[30] W. Huang, "Experimental studies for two-phase bubbly flow interfacial parameters in a horizontal channel," University of Wisconsin-Milwaukee, 1993.

[31] M. L. Lamari, "An experimental investigation of two-phase (air-water) flow regimes in a horizontal tube at near atmospheric conditions," Carleton University , Canada, 2001.

[32] R. C. B. a. S.-K. Yang, "EXPERIMENTAL INVESTIGATION OF TWO-PHASE BUBBLY FLOW PRESSURE DROP ACROSS A HORIZONTAL PIPE CONTAINING 90° BENDS," *CNL Nuclear Review,* pp. 1-15, 2016.

[33] Y. Y. Masayoshi SHIBA, "A Comparative Study on the Pressure Drop of Air-Water Flow," *Bulletin of JSME,* vol. 10, no. 38, pp. 290-298, 1967.

[34] T. O. M. E. Charles, "Vertical two-phase flow: Part II. Holdup and pressure drop," *The Canadian Journal of Chemical Engineering,* vol. 52, pp. 438-448, 1974.

[35] J. Zhou, "FLOW PATTERNS IN VERTICAL AIR/WATER FLOW WITH AND WITHOUT SURFACTANT," University of Dayton, 2013.

[36] I. Rand, "Airscout In-line User Manual," Ingersoll Rand, 2015.

[37] "TM Series Electronic Water Meters User Manual," Great Plains Industries, 2013.

[38] Grainger, "Digital Pressure Gauge," www.grainger.com.